AD NUMBER

AD-530 009

CLASSIFICATION CHANGES

TO UNCLASSIFIED

FROM CONFIDENTIAL

AUTHORITY

OCA; Dec 31, 1980 IAW Document Markings

19991029101

AD NUMBER

AD-530 009

NEW LIMITATION CHANGE

TO

DISTRIBUTION STATEMENT: A

Approved for public release; Distribution Unlimited.

LIMITATION CODE: 1

FROM DISTRIBUTION STATEMENT: B

LIMITATION CODE: 3

AUTHORITY

RADC Ltr; Nov 8, 1982

[redacted]

RADC-TR-73-370
Technical Report
March 1974

ACOUSTIC SOURCE LOCATION USING LONG BASE LINE TECHNIQUES (U)

Dr. James G. Constantine
1/Lt Mark D. Dickinson

Rome Air Development Center
Air Force Systems Command
Griffiss Air Force Base, New York

[redacted]

[redacted]

Do not return this copy. When not needed, destroy in accordance with pertinent security regulations.

[redacted]

AD-530 009 C

RADC-TR-73-370
ACOUSTIC SOURCE LOCATION USING LONG BASE LINE TECHNIQUES (U)
March 1974
Confidential Report

UNCLASSIFIED

ERRATA

June 1974

Please make the following insertion and correction to subject report:

1. Insert on the front cover:

"Classified by 692B SCG
Subject to GDS of EO 11652
Automatically downgraded at
two year intervals
Declassified on 31 Dec 1980"

2. In Block 15a of DD 1473, delete "GDS - Decl. 31 Dec 79" and insert "GDS - Decl. 31 Dec 1980"

Rome Air Development Center
Air Force Systems Command
Griffiss Air Force Base, New York

UNCLASSIFIED

SECURITY CLASSIFICATION OF THIS PAGE *(When Data Entered)*

REPORT DOCUMENTATION PAGE

READ INSTRUCTIONS BEFORE COMPLETING FORM

1. REPORT NUMBER: RADC-TR-73-370	2. GOVT ACCESSION NO.
3. RECIPIENT'S CATALOG NUMBER	
4. TITLE *(and Subtitle)*: ACOUSTIC SOURCE LOCATION USING LONG BASE LINE TECHNIQUES	5. TYPE OF REPORT & PERIOD COVERED: In-House (Mar. - Sep. 72)
	6. PERFORMING ORG. REPORT NUMBER: RADC-TR-73-370
7. AUTHOR(s): Dr. James G. Constantine 1/Lt Mark D. Dickinson	8. CONTRACT OR GRANT NUMBER(s): N/A
9. PERFORMING ORGANIZATION NAME AND ADDRESS: Rome Air Development Center (OCDE) Griffiss Air Force Base, New York 13441	10. PROGRAM ELEMENT, PROJECT, TASK AREA & WORK UNIT NUMBERS: Job Order No. 692B0205
11. CONTROLLING OFFICE NAME AND ADDRESS: Rome Air Development Center (OCDE) Griffiss Air Force Base, New York 13441	12. REPORT DATE: March 1974 13. NUMBER OF PAGES: 48
14. MONITORING AGENCY NAME & ADDRESS *(if different from Controlling Office)*: Same	15. SECURITY CLASS. *(of this report)*: Confidential 15a. DECLASSIFICATION/DOWNGRADING SCHEDULE: GDS – Decl. 31 Dec. 80

16. DISTRIBUTION STATEMENT *(of this Report)*

Distribution limited to US Gov't agencies only; foreign info [redacted]; March 1974. Other requests for this document must be referred to RADC (OCDE), GAFB, NY 13441.

17. DISTRIBUTION STATEMENT *(of the abstract entered in Block 20, if different from Report)*

Same

18. SUPPLEMENTARY NOTES

None

19. KEY WORDS *(Continue on reverse side if necessary and identify by block number)*

Cross-Correlation
Auto-Correlation
Acoustic Detection
Acoustic Signatures
Tracking (Position)

20. ABSTRACT *(Continue on reverse side if necessary and identify by block number)*

UNCLASSIFIED ABSTRACT

A study is made of acoustic base line methods for detecting and locating surface sound sources such as trucks. The experimental system used is composed of widely separated omnidirectional receivers and a signal processor which operates on the receiver outputs. The long base lines and the highly periodic nature of the acoustic signals generated by engines of any type lead to severe ambiguity in acoustic source location. Mathematical derivations and experimental analysis have led to signal processing techniques which reduce the periodic components of the source signals and preserve the random signal components for use in time-of-arrival

DD FORM 1 JAN 73 1473 EDITION OF 1 NOV 65 IS OBSOLETE

UNCLASSIFIED

SECURITY CLASSIFICATION OF THIS PAGE *(When Data Entered)*

20. ABSTRACT (continued)

measurements. Subsequent source location is highly successful. In the present analysis: (a) a source whose sound-pressure level (SPL) is about 100 dB re 0.0002 microbar and whose signal contains strong periodic components was detected and located using base lines of about 1000 meters; (b) accuracies in locating the sound source of several meters were achieved under calm weather conditions; and (c) identification of the sound sources was successfully performed based on spectral signatures.

SUMMARY

A study is made of acoustic base line methods for detecting and locating surface sound sources such as trucks. The experimental system used is composed of widely separated omnidirectional receivers and a signal processor which operates on the receiver outputs. The long base lines and the highly periodic nature of the acoustic signals generated by engines of any type lead to severe ambiguity in acoustic source location. Mathematical derivations and experimental analysis have led to signal processing techniques which reduce the periodic components of the source signals and preserve the random signal components for use in time-of-arrival measurements. Subsequent source location is highly successful. In the present analysis: (a) a source whose sound-pressure level (SPL) is about 100 dB re 0.0002 microbar and whose signal contains strong periodic components was detected and located using base lines of about 1000 meters; (b) accuracies in locating the sound source of several meters were achieved under calm weather conditions; and (c) identification of the sound sources was successfully performed based on spectral signatures.

PREFACE

The study described in this report was accomplished in-house in the Surveillance Equipment Development Branch of Rome Air Development Center, under Job Order Number 692B0205.

This report contains classified information extracted from the two classified documents asterisked in the References.

The authors wish to express their gratitude to Lt Col R.C. Salisberry and Mr. E.F. Krzysiak of RADC for their suggestions in analyzing the technical data and for their support during this effort. They also wish to thank Capt D. Hammond and Mr. M. Crone, both formerly of RADC, for their contributions in signal processing and for writing many of the computer programs.

This technical report has been reviewed and is approved.

APPROVED:

JOSEPH M. EANNARINO
Chief, Surveillance Equipment Development Branch
Surveillance & Control Division

APPROVED:

WILLIAM T. POPE
Assistant Chief
Surveillance & Control Division

FOR THE COMMANDER:

CARLO P. CROCETTI
Chief, Plans Office

TABLE OF CONTENTS

		PAGE
I.	INTRODUCTION	7
II.	THEORY	8
	A. Correlation Analysis	8
	B. Time-of-Arrival Techniques	9
	C. Signal Prewhitening	10
	D. Spectral Analysis	11
III.	EXPERIMENTAL APPARATUS AND EXPERIMENTAL ARRANGEMENT	12
	A. Target-Sensor Configuration	12
	B. Sensor System Description (Phase III Commikes)	12
	C. RADC Acoustic System	16
	1. Sound System	16
	a. Broad Band Noise	16
	b. Swept Tones	16
	c. Moving Target (Truck)	17
	d. Interfering Targets	17
	2. Microphones	17
	3. Micrometeorological Instrumentation	17
	4. Recording Equipment	17
IV.	ANALYSIS AND RESULTS	18
	A. Spectrum Analysis	18
	1. Sound Intensity	18
	2. Source Spectrum	18
	B. Correlation Analysis	21
	1. Results and Interpretation	23
V.	SUMMARY AND CONCLUSIONS	40
	References	43
	APPENDIX	A-1

FIGURES

FIGURE NO.	TITLE	PAGE
1.	Location of a Sound Source by Triangulation	9
2.	Source and Sensor Locations at Auxiliary Field Nc. 6 Eglin AFB FL	13
3.	Microphone Arrays (All Distances in Meters)	14
4.	Phase III Commike Modification for PAVE ONYX Mission	15
5.	S-Band Data Link for Phase III Commikes	16
6.	The Power Spectrum of: (a) the generator in the analysis range 0-2000 Hz, 0 dB gain; (b) the generator in the analysis range 100-2000 Hz, 20 dB gain; and (c) the background noise (generator off) in the analysis range 0-2000 Hz, 20 dB gain. (Array No. 2)	19
7.	The Power Spectrum of the Generator for Different Microphones in the Analysis Range of 0-100 Hz; (a) in the direction of the exhaust, exciter-on; (b) in the direction of the exhaust, exciter-off; (c) behind the exhaust, exciter-on; (d) behind the exhaust, exciter-off	20
8.	Time Waveform Generated by the Source as Recorded at the Four Microphones of Array Number 2.	22
9.	Time Waveform Generated by the Source: (a) exciter-on; (b) exciter-off	23
10.	Time Series Spectrum of the Source Signal: (a) exciter-on; (b) exciter-off	24
11.	Cross-correlation Function of M1 vs M2: (a) source signal; (b) 40-80 Hz band-limited white noise; and (c) 40-150 Hz swept tones.	25
12.	Cross-correlation Function of M1 vs M3: (a) source signal; (b) 40-80 Hz band-limited white noise; and (c) 40-150 Hz swept tones	26
13.	Cross-correlation Function of M1 vs M4: (a) 40-80 Hz band-limited white noise; (b) 40-150 Hz swept tones; and (c) source signals	27
14.	Cross-correlation Function of M2 vs M3: (a) source signals; (b) 40-80 Hz band-limited white noise; and (c) 40-150 Hz swept tones	28
15.	Cross-correlation Function of M2 vs M4: (a) source signals; (b) 40-80 Hz band-limited noise; and (c) 40-150 Hz swept tones	29
16.	Cross-correlation Function of M3 vs M4: (a) source signals; (b) 40-80 Hz band-limited noise; and (c) 40-150 Hz swept tones	30

FIGURES (Cont'd.)

FIGURE NO.	TITLE	PAGE
17.	Auto-correlation of 100-1000 Hz band-limited: (a) source signal; (b) background noise	32
18.	Cross-correlation Function of M3 vs M4 (Array No. 4) over the Analysis Range 0-500 msec. Band-Limited Source Signals: (a) 100-1000 Hz; (b) 150-1000 Hz; (c) 50-1000 Hz; and (d) band-limited white noise 160-320 Hz	33
19.	Normalized Cross-correlation M2 vs M3 of Unwhitened Source Signals (τ=28 msec)	34
20.	Normalized Cross-correlation M2 vs M3 of Log-Whitened Source Signals	35
21.	Cross-correlation Between M3 and M4, after Signal Prewhitening, as a Function of the Integration Windows: (a) 1/4 sec window; (b) 1/2 sec window; (c) 1 sec window; (d) 4 sec window	37
22.	Time Series Spectrum of the Source Signal Using Data Obtained from an Operational System (Eglin AFB)	38
23.	Cross-correlation Function of Source Signals after Prewhitening Using the IGLOO WHITE System	39
24.	Block Diagram of Digital Prewhitening Technique as Applied to the Cross-Spectral Power Density	A-3

TABLE

TABLE NO.		PAGE
I	Correlation Analysis (Array No. 4)	31

I. (U) Introduction

The purpose of this work was to assess experimentally the feasibility of locating power generators by time-correlating their acoustic energy relayed by three or more spatially-separated acoustic sensors. Correlation techniques are very commonly used in the process of localizing noise sources[1-11] and many of the factors affecting sound-ranging are well understood[12].

The specific problem addressed in this work was eliminating the spurious maxima from the correlation function of the generator signal. These spurious maxima result from the dominant periodic components existing in the generator's acoustic signal. Depending on the nature of the sensor configuration and the particular generator tested ten or more maxima of equal amplitude may appear in the correlation function. This makes it difficult to correctly identify the true correlation maximum.

This report discusses a successful technique to eliminate the effect of periodic components from the correlation function and defines relatively simple methods of correctly identifying these types of targets. Chapters II, III, IV, and V, respectively, discuss the theory behind this experiment, the experimental apparatus and microphone configuration, the experimental analysis and results, and summarize the findings.

II. (U) Theory

The location of sound sources is done by using time-of-arrival techniques. To establish the coordinates of the acoustic source by this method the following must be known: (a) a minimum of two independent delay times (time differences between the same event received at several microphone locations); and (b) the corresponding microphone separating distances (base lines). In practice, the microphone array configuration is known and the only parameters to be measured are the delay times between the elements of at least a three-microphone array. If the acoustic source is of impulsive nature the time difference between signals received at several microphone locations is easily defined. This, however, is not so in the case of continuous signals. In the latter case cross-correlation techniques can achieve results analogous to those obtained for the pulse case.

A. Correlation Analysis

The cross-correlation of two waveforms is a measure of their similarity as a function of the time shift between them. Mathematically this can be achieved by computing the cross-correlation function. That is, the two signals are multiplied and summed over a specified time window T. This is done for different values of time τ. For the value of τ at which the two signals match, a maximum value of the correlation function is obtained. This value of τ is equal to the delay time of one signal relative to the other. The mathematical expression for the discrete cross-correlation function is:

$$R_{ij}(m,k) = \frac{1}{N} \sum_{n=m}^{N+m} X_i(n)\, X_j(n-k) \qquad (1)$$

Here, $X_i(n)$ is the signal on channel i at the n^{th} sample instant, $X_j(n-k)$ is the signal on channel j at the (n-k)th sample instant, k is the delay between channels in samples, N is the correlation window in samples, and m is the sample instant for start of the correlation window.

In the case of discrete plotting of a series of measurements in the form of pairs of observation points $X_i(n)$ and $X_j(n)$, a normalized measure of correlation lying between -1 and +1 is often desirable. The digital form of the normalized correlation is:

$$\rho_{ij}(m,k) = R_{ij}(m,k) \cdot \left[\left[\frac{1}{N} \sum_{n=m}^{N+m} X_i^2(n) \right] \cdot \left[\frac{1}{N} \sum_{n=m}^{N+m} X_j^2(n) \right] \right]^{-1/2}$$

The normalized correlation function was suggested as a method to reduce spurious correlation maxima. The rationale behind it is as follows: Write Eq (1) as,

$$R_{ij}(m,k) = \sigma_i(m)\, \sigma_j(m-k)\, \rho_{ij}(m,k)$$

where,

$$\sigma_i(m) = \left[\frac{1}{N} \sum_{n=m}^{N+m} X_i^2(n) \right]^{1/2} \qquad (4)$$

If there is a large change in energy in the signal from one correlation record to the next, then it is possible that,

$$R_{ij}(m_1,k_1) > R_{ij}(m_2,k_2) \qquad (5)$$

while,

$$\rho_{ij}(m_1, k_1) < \rho_{ij}(m_2, k_2) \tag{6}$$

simply because

$$\sigma_i(m_1)\,\sigma_j(m_1 - k_1) >> \sigma_i(m_2)\,\sigma_j(m_2 - k_2) \tag{7}$$

If the signal is quasi-stationary in the sense that its spectral shape does not change with time, then ρ_{ij} will be independent of the record time m. Hence it will be a more consistent estimator of the true correlation maxima than R_{ij} if the signal energy, above, is non-stationary.

For an example, consider the application of correlation techniques to an acoustic receiving system consisting of a three-element array. The coordinates of the array relative to a known origin, in this case a control processing center, will be known.

B. Time of Arrival Techniques

In Figure 1 the field deployment of such an array is illustrated. It has been mentioned above that the signal from the source, whose position relative to the array is S (X,Y), arrives at different times at M1, M2, and M3. The difference in time-of-arrival (delay time τ) can be determined using cross-correlation techniques. Using the delay time to locate the source of disturbance one must find a relationship between τ and the geometry of the system. To simplify the calculations we have assumed a planar geometry (i.e., $Z=Z_1=Z_2=Z_3$). If this is not the case an array of at least four sensors is required to locate the sound source.

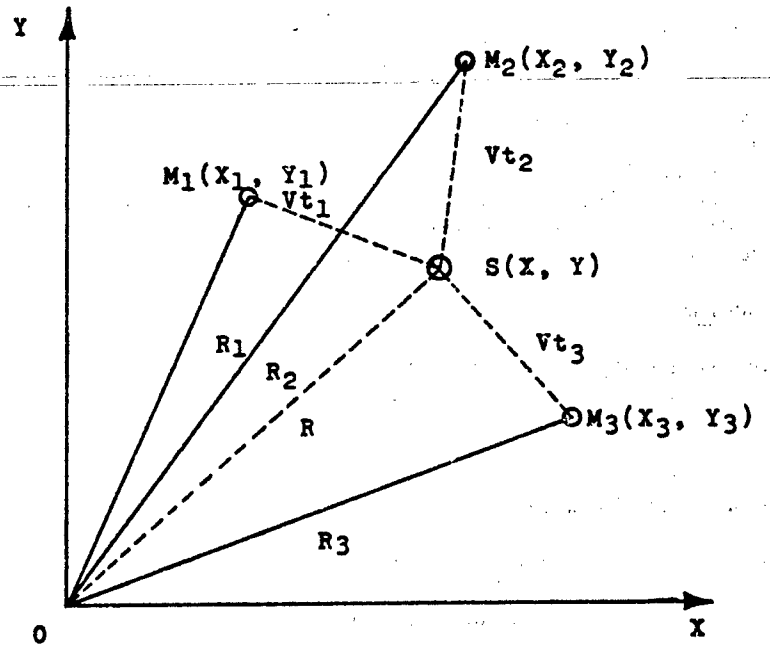

Figure 1. Location of a Sound Source by Triangulation

Using an orthogonal coordinate system the microphone configuration can be designated as M1(X_1, Y_1), M2(X_2, Y_2), and M3(X_3, Y_3). Using simple geometrical configurations the following relationships can be obtained for the time delays of the signal produced by an acoustic source S having coordinates (X, Y) and recorded at M1, M2, and M3:

$$\tau_{12} = t_1 - t_2 = \frac{1}{V}\left[\left[(Y_1-Y)^2 + (X-X_1)^2\right]^{1/2} - \left[(Y_2-Y)^2 + (X_2-X)^2\right]^{1/2}\right],$$

$$\tau_{13} = t_1 - t_3 = \frac{1}{V}\left[\left[(Y_1-Y)^2 + (X-X_1)^2\right]^{1/2} - \left[(Y-Y_3)^2 + (X_3-X)^2\right]^{1/2}\right], \quad (8)$$

and

$$\tau_{32} = t_3 - t_2 = \frac{1}{V}\left[\left[(Y-Y_3)^2 + (X_3-X)^2\right]^{1/2} - \left[(Y_2-Y)^2 + (X_2-X)^2\right]^{1/2}\right].$$

In the above equation V is the velocity of sound in the atmosphere and is given by:

$$V = V_o \cdot \sqrt{\frac{T}{T_o}} + V_w \quad (9)$$

Here V_o = 332 meters per second at 0 °C, T is the absolute temperature in degrees kelvin, T_o is the ambient temperature in degrees kelvin and V_w is the velocity of the wind.

Equations 8 are the equations of hyperbolas whose foci are the fixed points M1, M2, and M3. Therefore, for a given τ we can determine a hyperbola, that is a set of points whose difference in distance from the fixed points, for example, M1 and M2, is equal to τ_{12} (a constant). Two such hyperbolas should intersect at least once. The point of intersection determines the location of the source of disturbance. As the source changes position the delay times will also change and hence a new intersection will be defined. Therefore, by computing the delay times between different microphone pairs in real time the source of disturbance can be tracked.

C. Signal Prewhitening

Signal prewhitening is used primarily to reduce the periodic structure of the correlation function.[10] In the present analysis the prewhitening and cross-correlation scheme consists of taking two time functions $X_1(t)$ and $X_2(t)$, taking the discrete Fourier transforms $F_1(w)$ and $F_2(w)$, multiplying the first with the conjugate of the second in order to find the cross-spectral power density, prewhitening the result in order to suppress periodicity, and then taking the inverse transform to obtain the cross-correlation. Note that if the prewhitening step is omitted the result is a normal cross-correlation function.[13]

For example, if $X_1(t)$ and $X_2(t)$ are two time functions their Fourier transforms $F_1(\omega)$ and $F_2(\omega)$ can be written:

$$F_1(\omega) = a_1(\omega) + j\, b_1(\omega)$$

and

$$F_2(\omega) = a_2(\omega) + j\, b_2(\omega) \quad (10)$$

Then the cross-spectral power density is:

$$S_1, 2(\omega) = F_1(\omega)\, F^*_2(\omega) = [a_1(\omega)\, a_2(\omega) + b_1(\omega) b_2(\omega)]$$

$$+ j[a_2(\omega)\, b_1(\omega) - b_2(\omega) a_1(\omega)].$$

Any prewhitening scheme in the frequency domain can be considered to be a multiplication of $S_{1,2}(\omega)$ by a function $K^2(\omega)$.[10] In general, there are no restrictions placed on $K^2(\omega)$. However, in order to preserve phase information, $K^2(\omega)$ is required to be positive real. After performing the multiplication we have,

$$T_{1,2}(\omega) = S^{(\omega)}_{1,2} K^2(\omega) \tag{11}$$

where,

$$K^2(\omega) = \frac{\ell n(\alpha^2 + \beta^2)}{2[\alpha^2+\beta^2]^{1/2}} \tag{12}$$

here,

$$\alpha = 1_1(\omega)\, a_2(\omega) + b_1(\omega)\, b_2(\omega) \text{ and}$$

$$\beta = a_2(\omega)\, b_1(\omega) - b_2(\omega)\, a_1(\omega) \tag{13}$$

At this point take the inverse transform of $T_{1,2}(\omega)$. Using the convolution theorem the inverse transform of $T_{1,2}(\omega)$ equals the inverse transform of $S_{1,2}(\omega)$ convolved with the inverse transform of $K^2(\omega)$. Then since the inverse transform of $S_{1,2}(\omega)$ is the cross-correlation $R_{1,2}(\tau)$ of $X_1(t)$ and $X_2(t)$, the result is the corss-correlation of $X_1(t)$ and $X_2(t)$ convolved with a function $k(\tau)$, where $k(\tau)$ is the inverse transform of $K^2(\omega)$.

D. Spectral Analysis

Spectral analysis is based upon computation of the Fourier integral:

$$S_X(f) = \int_{-\infty}^{\infty} X(t) \exp(-2\pi f t)\, dt \tag{14}$$

In order to understand how computation of the Fourier integral helps to make meaningful measurements, consider the Fourier transform written in its sine-cosine form:

$$S_X(f) = \int_{-\infty}^{\infty} X(t)(\cos 2\pi f t - j \sin 2\pi f t)\, dt \tag{15}$$

This equation states that the transform averages a time function input X(t) with a set of sines-cosines to determine the content of X(t) at some frequency f. Thus the transform resolves the time function into a set of components at various frequencies much as a set of analog filters would. However, it not only yields the amplitude of each frequency, but also resolves the in-phase (real, cosine) component and the quadrature (imaginary, sine) component, thereby giving magnitude and phase information which is difficult to obtain in any other way.

III. (U) Experimental Apparatus and Experimental Arrangement (U)

A.(C)Target – Sensor Configuration (U)

(C) The target, 50 Hz, 75 KVA generator motor set, was tested in a semi-jungle environment area on Auxiliary Field No. 6 at Eglin AFB, Florida. The test was conducted in order to establish criteria for locating and identifying generator type targets. Figure 2 depicts the relationship between the sound source and the sensors. The detection system consisted of modified Phase III commikes (MCOM), hand-emplaced commikes (HEC), and an RADC acoustic system. The Phase III commikes were connected to a central recording station via an RF link, while the RADC microphones were hard-wired into a recording system.

(C) The MCOM and HEC were placed at points designated by stake markers on the four legs (north, south, east, and west) from the source. The stakes were in 100-meter increments up to 1 kilometer and from there in 500-meter increments up to 2 kilometers. The source as indicated in Figure 2 was positioned off-center. The location was approximately 20 meters from center on the north leg and approximately 8 meters from center on the west leg. It should be noted that the exhaust was directed parallel to the east leg.

(C) The two MCOMS and one HEC were collocated on each of the four legs. Two MCOMS allowed for backup data in case a MCOM failed during a test. The HEC gave continuous audio data for evaluation of the audio signal at any time during the operation of the MCOMS.

(C) The RADC acoustic microphones were positioned at various points along the four legs of the test array. Figure 3 depicts the four different arrays used by RADC and the positions of the microphones relative to the source.

B.(C) Sensor System Description (Phase III Commikes) (U)

(C) The HEC transmitted continuous audio while the MCOM transmitted type I messages upon recognition of the source. The MCOM was commanded to the audio mode at various times throughout the test. The MCOM consists of a Phase III commike modified by NADC (Naval Air Development Center). The commike was modified to consist of detection circuitry which was included in the audio module,[14] as shown in Figure 4.

(C) The detection circuitry consisted of a phase lock loop which sweeps from 72 to 78 Hz nominal. A signal within this frequency range must be present at least 10 seconds (enable timer) before the unit will begin to process the signal. After the 10-second period, the signal must be present for 7 minutes more (verification timer), with no dropouts exceeding 10 seconds. At the end of 7 minutes a type I message is transmitted signifying the presences of the "source." If the signal should dropout for more than 10 seconds the entire process starts over with the enable timer. At any time during the processing of the signal the MCOM can be commanded into the audio mode.

(C) There is a certain finite amount of time during which any MCOM can transmit audio after being commanded into the audio mode. The amount of continuous audio time after a command to the audio mode is 20 seconds nominal. Since the unit's battery life is limited mainly by the number of times it transmits audio, the audio command is used infrequently.

(C) The operating characteristics of the MCOM are the same as the Phase III commike but will be restated here for clarity. The frequency response of the MCOM is from 50 to 2 KHz with output distortion less than 10% for the audio mode. The output noise level is 24 millivolts rms maximum while the instantaneous dynamic range is 32 db.

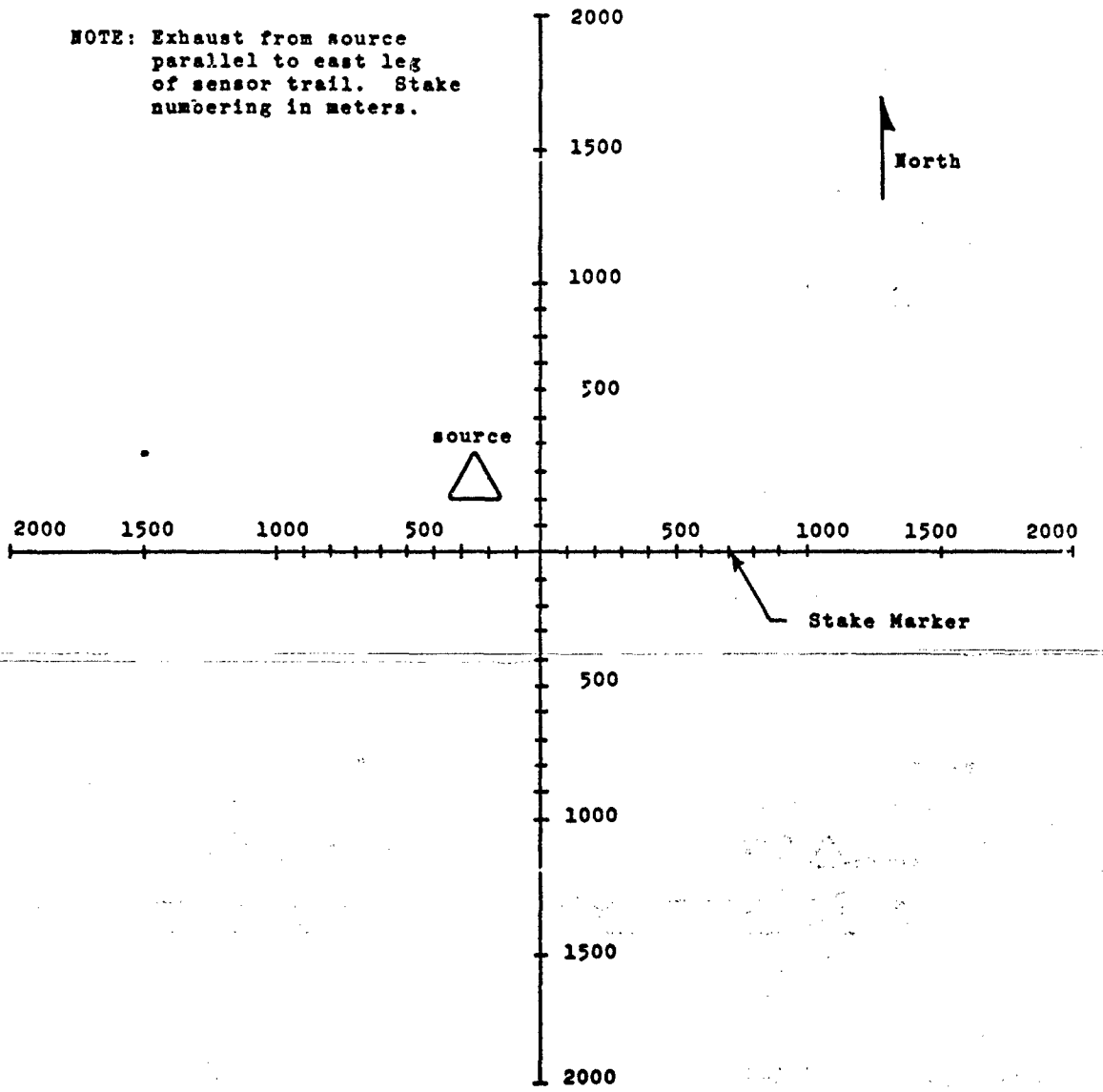

Figure 2. Source and Sensor Locations at Auxiliary Field No. 6 Eglin AFB FL

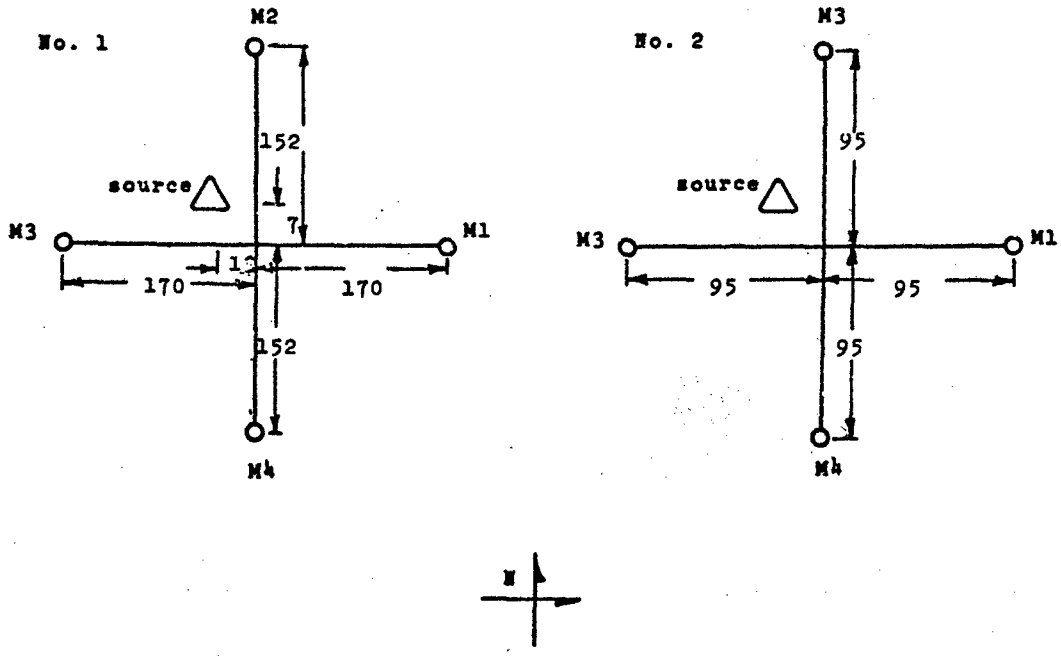

Figure 3. Microphone Arrays (All Distances in Meters)

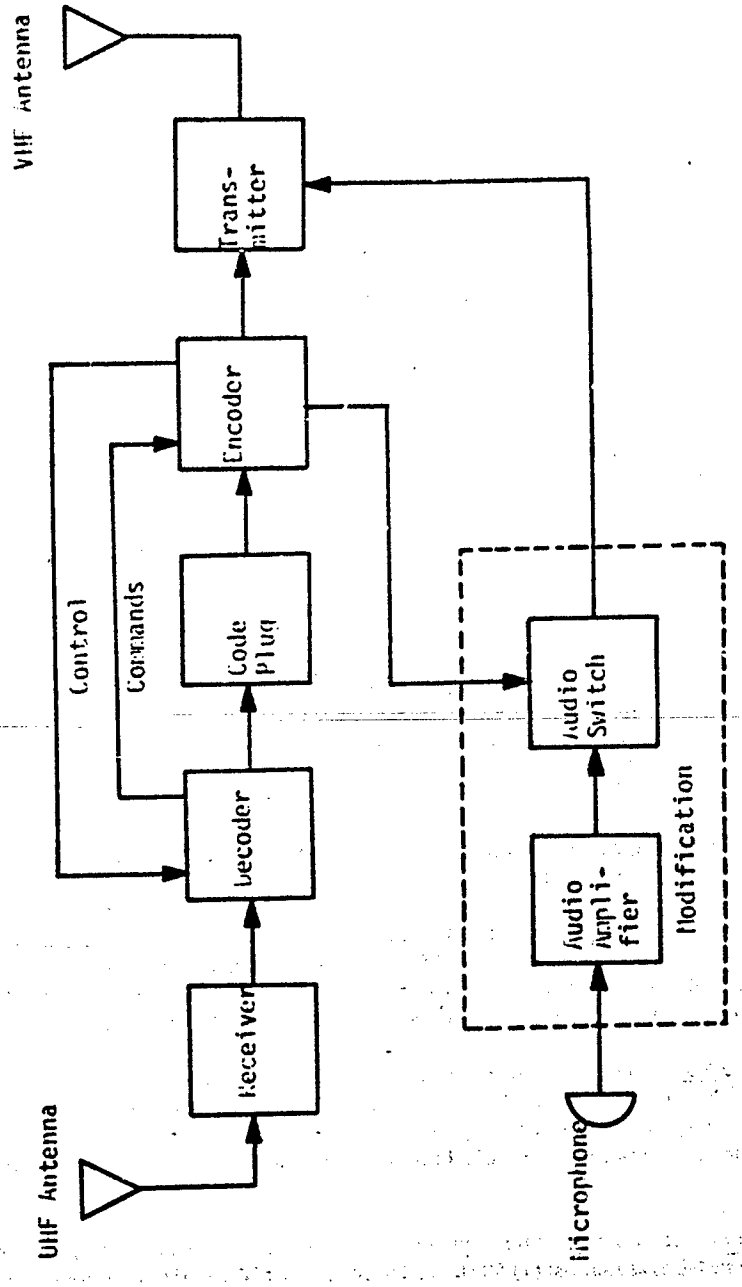

Figure 4. Phase III Commike Modification for PAVE ONYX Mission

(C) The information transmitted by the MCOM is received, digitized, and transmitted (S-band) by an airborne segment data link to a receiving and analysis center. The digitizing rate is approximately 4 KHz. The digital information is then transmitted using an S-band transmission. The link is depicted in Figure 5. The audio digital data is then transformed back to analog data (D/A) at the receiving and analysis center.

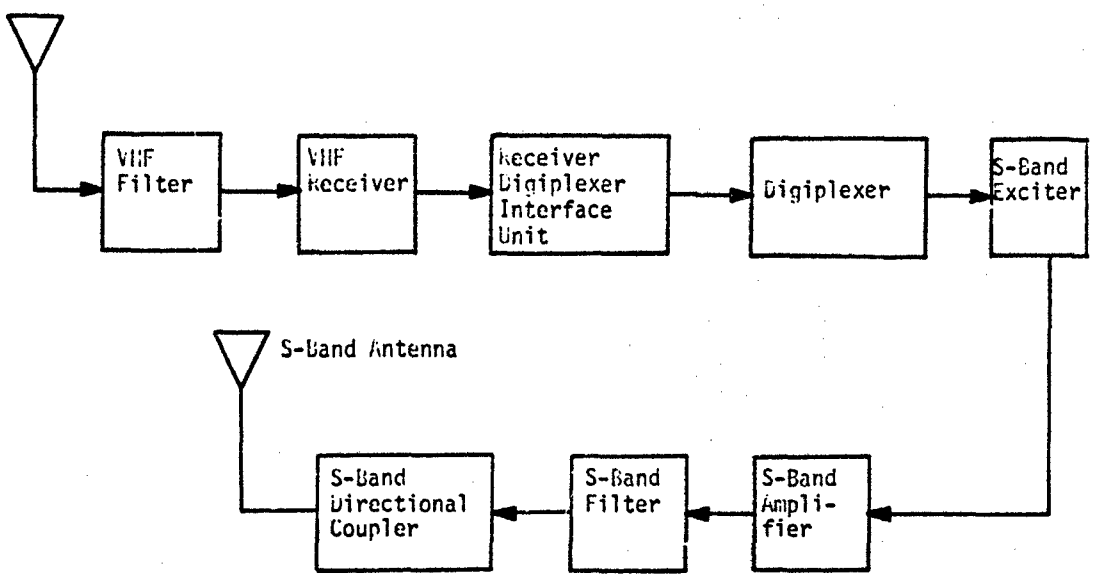

Figure 5. S-Band Data Link for Phase III Commikes

C. (U) RADC Acoustic System

The RADC experimental apparatus consisted of the sound system, microphones, the micrometeorological instrumentation, and the recording equipment.

1. Sound System – The sound system was a 100-watt system consisting of two loudspeakers and an audio tape recorder. The speakers were Lansing Models LE 154 which have a relatively flat response in the frequency range 40-6000 Hz. The audio portable recorder was a Tandberg Model 11 with frequency response 40-20,000 Hz. In addition to the generator target the following sound sources were used in this experiment:

a. Broad Band Noise – Filtered noise in octave bands were used as a noise source. The bands are 40-80 Hz, 80-160, 160-320, 320-640, 640-1280 Hz. The duration of these signals is 15 seconds each. These signals were used to determine the ability to cross-correlate on pure noise and to compare these results with cross-correlation functions obtained from the "source truck" signals. In addition to noise-like signals, truck signatures contain strong spectral lines.

b. Swept Tones – These are swept tones and pure tones covering the frequency range between 50-150 Hz. The structure of these signals is as follows: (1) 50 Hz for 15 seconds; (2) 50-150 Hz range swept in 15 seconds; (3) 150-50 Hz swept in 15 seconds; (4) 50 Hz pure tones for 15 seconds. These signals were included in order to make direct comparison with the source signals which appear to sweep the same frequency range. Also, it was of interest in itself to test cross-correlation on these types of signals.

c. Moving Target (Truck) – The signatures from a moving truck along a prescribed path have been recorded. These signatures were used as an interfering target.

d. Interfering Targets

(1) In this case three trucks were used at the same time. The trucks were separated by 100m.

(2) Prop and jet aircraft were used as interfering targets in various configurations. The masking experiments are designed to determine the effectiveness of cross-correlation techniques to locate and follow targets of interest as a function of base line in the presence of interference phenomena.

2. Microphones – In answering the question concerning the applicability of cross-correlation techniques for a stationary periodic target, four arrays of microphones were used. These are depicted in Figure 3. An array consisted of four omnidirectional microphones. The microphones are GR-P1560-9531's and have a frequency response which is flat in the range between 2 and 6000 Hz.

3. Micrometeorological Instrumentation – A meteorological system manufactured by Meteorology Research, Inc. (MRI) was used in this experiment. The instrumentation was mounted on a 6-foot tower. The system is capable of giving the temperature, wind speed, and wind direction. Using these data, information about temperature stability and the turbulence in the area can be obtained.

4. Recording Equipment – The signals from the microphones are hardwired to a central recording system. The lines are driven by a set of amplifiers which are gain switchable. The total dynamic range of the system is 90 db and the gain can be switched between 27 db and 97 db. The steps are 10 db each. The bandwidth of the system is 2 to 2000 Hz. The output of the amplifiers was fed into a 14-channel analog tape recorder. The recorder was a Honeywell 5600 magnetic tape recorder. Out of the 14 channels in the FM record mode four were used for the microphones and three were used for the meteorological channels. The edge track A was used for voice commentary.

IV. (U) Analysis and Results

The experimental data for this effort were collected at Eglin AFB Florida. The experimental details and the type of the sound source (referred to as "source" in the following sections) against which the data were collected are summarized in Chapter III of this report. The analysis of the data was performed by using the following equipment: (a) Federal Scientific Correlation and Probability Analyzer; (b) Federal Scientific UA-6B Spectrum Analyzer; and (c) PDP-9 General Purpose Digital Computer.

A. Spectrum Analysis

To determine the properties of the "source," its sound intensity and the frequency spectrum of the emitted signal were examined.

1. Sound Intensity – To establish a safe distance over which the "source" could be detected the sound-pressure level (SPL) one meter away from the target was examined. The SPL at any distance from the sound source can be determined using the following relationship:[15], [16], [17]

$$I(R) = (W_S + D) - 20 \log R - MR - T \text{ (dB)} \qquad (16)$$

Here, W_S is the source acoustic power in dB relative to 10^{-16} watts; D is the directivity index; M is the attenuation coefficient in dB per unit distance; and T is the transmission loss in dB. The term 20 log R represents the geometrical spreading loss.

The "source" exhibited some degree of directionality. The SPL one meter away and in the direction of the exhaust system, or the two sides adjacent to the exhaust, was found to be 108 dB, while the SPL on the side opposite to the exhaust was about 100 dB. The background noise at the test site was of the order of 56 dB during the day and about 40 dB during the night. The Eglin terrain was heavily wooded and a loss coefficient[17] M = .0264 dB/m is estimated for this terrain and for this source (i.e., most of the energy of the source is found to be below 150 Hz).

Using Equation (16), the SPL of the "source," and the environmental noise, an effective range for a signal-to-noise ratio equal to unity is: (a) in the direction of the exhaust: (1) daytime, R=340m and (2) nighttime, R=460m; (b) in a direction opposite to the exhaust: (1) daytime, R=230m and (2) nighttime, R=380m. These results are in excellent agreement with the experimentally observed values. However, data processing improved the above detection ranges considerably (i.e., a factor of two or more is a realistic range with minimum processing).

The above analysis shows that a safe range for detecting the source of interest, with minimum data processing, is about 600m. Larger ranges could be achieved if the background noise is reduced and/or by additional processing of the data. The periodic nature of the source of interest (see next section) suggests that ranges of several kilometers could be achieved by averaging the data over longer periods of time (i.e., several minutes).

2. Source Spectrum – Using Equation (14) the spectrum of the source signal has been calculated. In Figure 6. a. a typical power spectrum over an analysis range 0-2000 Hz is shown. In Figure 6.b. the source spectrum is shown over the analysis range of 100-2000 Hz after the signal was amplified by 20 dB. This chart was produced by passing the signal through a high pass filter and then amplifying it by 20 dB. Figure 6.c. shows the power spectral density of the background noise (generator off), produced under the same conditions as Figure 6.b. In addition to the fact that the source is highly periodic, Figure 6 indicates that most of the acoustic energy is found in the 0-100 Hz frequency band. Figure 7 shows details of the generator spectrum in this frequency range. It is observed that the signal has a fundamental of 12.5 Hz and that the strongest frequency component is at 25 or 37.5 Hz (i.e., the second or the third harmonic). Whether the 25 Hz or the 37.5 Hz line is the strongest line in the spectrum depends

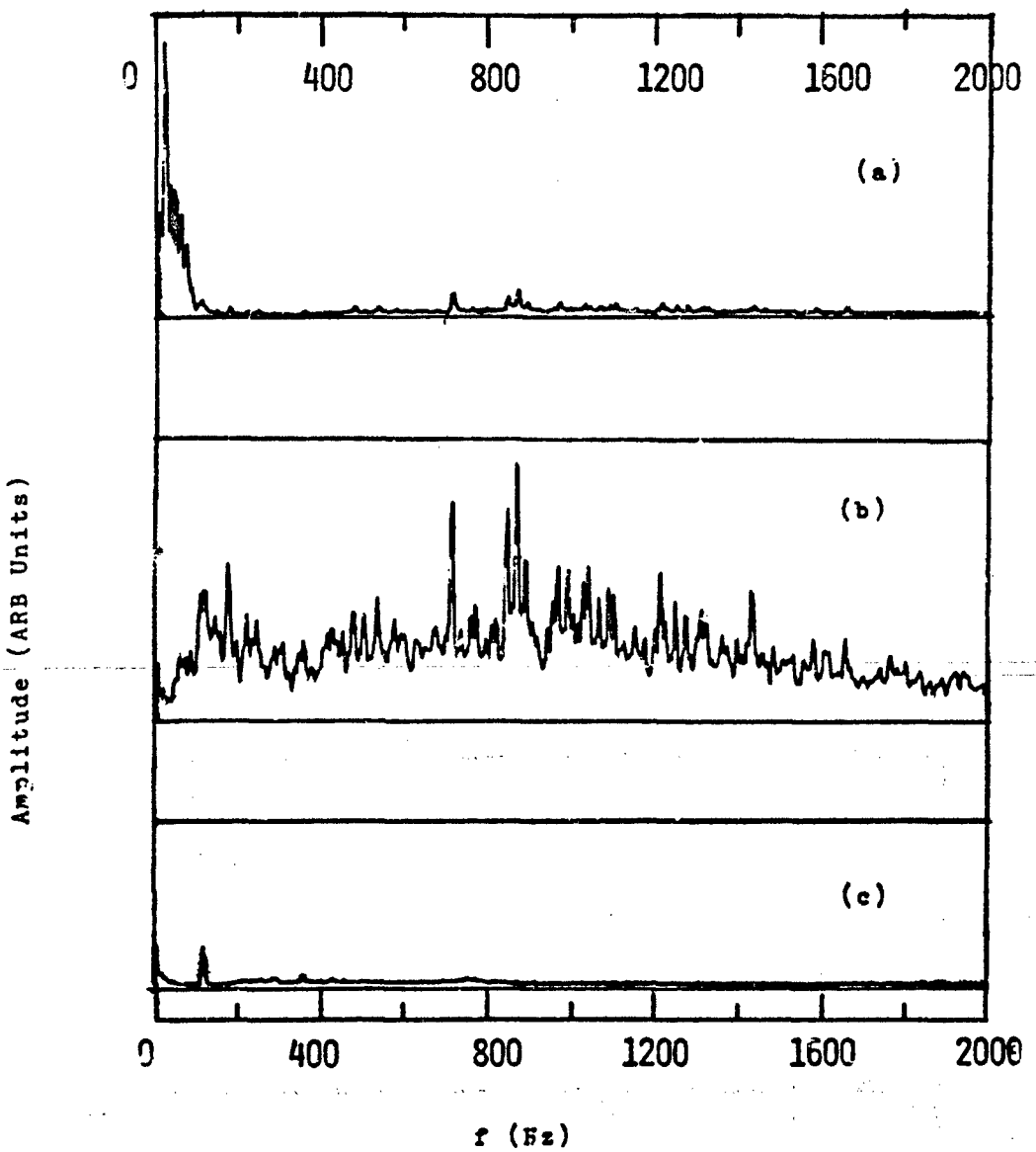

Figure 6. The Power Spectrum of: (a) the generator in the analysis range 0-2000 Hz, 0 dB gain; (b) the generator in the analysis range 100-2000 Hz, 20 dB gain; and (c) the background noise (generator off) in the analysis range 0-2000 Hz, 20 dB gain. (Array No. 2)

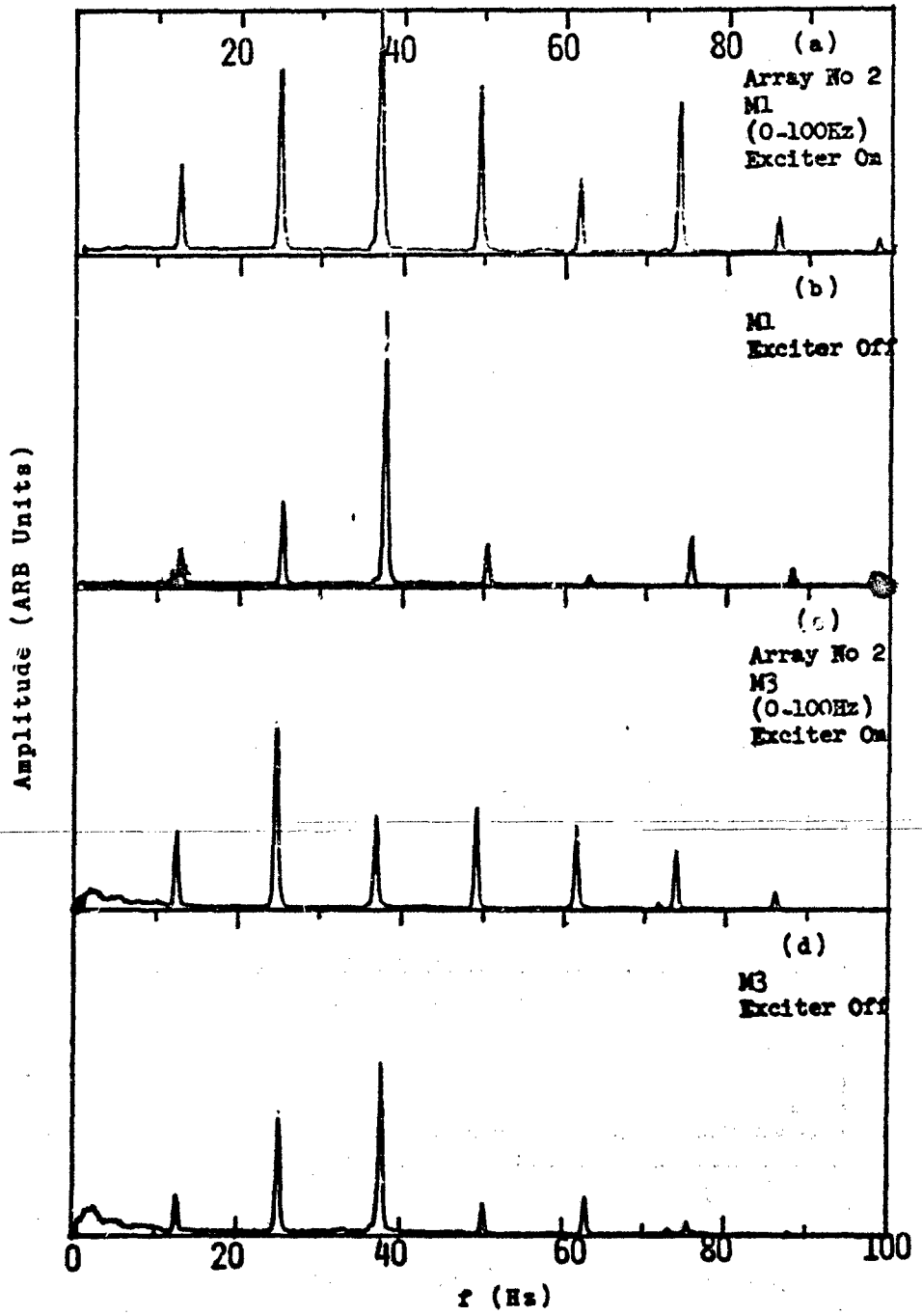

Figure 7. The Power Spectrum of the Generator for Different Microphones in the Analysis Range of 0-100 Hz; (a) in the direction of the exhaust, exciter-on; (b) in the direction of the exhaust, exciter-off; (c) behind the exhaust, exciter-on; (d) behind the exhaust, exciter-off.

on the direction of the exhaust pipe relative to the detector. That is, if the microphone is in the same direction as the exhaust pipe outlet, the 37.5 Hz line is the strongest line in the received spectrum, while if the microphone is in the opposite direction to the exhaust pipe outlet, the 25 Hz line is the strongest.

From the mechanics of the source, the 12.5 Hz line appears to be associated with the cylinder firing rate. The cylinder firing rate (CFR) for a six-cylinder, four-cycle engine is given by:[18]

$$CFR = \frac{RPM}{2x60} = \frac{[\text{Revolutions Per Minute}]}{\left[60\ \frac{\text{sec}}{\text{min}}\right] x\ 2} \quad (\text{Hz}) \qquad (17)$$

The engine tested had an RPM=1500. From Equation (17) one sees that the CFR=12.5 Hz. The 12.5 Hz line appears to be modulating all its harmonics. This modulation is clearly seen in the time function Figure 8, where the two adjacent peaks are 80 milliseconds apart. This is a distinct characteristic of this type of sound source and can be used to correctly identify it. Less than one second of data is required to correctly classify the target. Notice, however, that the 12.5 Hz modulation is reduced when the source is running with no load on (i.e., when the exciter is turned off). A direct comparison of the time function of the source with the exciter on and the exciter off is shown in Figure 9. Figure 10 shows a typical time series spectrum of the source with the exciter on and the exciter off. When the exciter is off the lines are shifted slightly into higher frequency (see also Figure 7). The behavior of the source with the exciter on/off is not well understood. Puzzling also is the fact that the 25 or 37.5 Hz line is more intense than the engine firing rate (EFR), which in this case is given by:[18]

$$EFR = \frac{(RPM \times (6\ cyl))}{\left[60\ \frac{\text{sec}}{\text{min.}}\right] X\ 2} = \frac{1500 \times 6}{60 \times 2\ (\text{sec})} = 75\ \text{Hz} \qquad (18)$$

This may be due to the mechanics of the muffler. No data have been collected with the muffler off using this experimental apparatus to verify this assumption.

Another important feature of the source is shown in Figure 6. In this figure, although there is significant energy in the frequency domain between 100-2000 Hz this energy is about 20 dB less than the energy found between 0-100 Hz. However, randomness in the source signal is more pronounced in the analysis range 100-2000 Hz.

From the above it is concluded that the class of targets can be easily identified on the basis of the modulation associated with the cylinder firing rate and/or using the rich harmonic content and periodic nature of the source spectrum. Also the fact that there is enough randomness in the source signal allows it to be used as a basis for correlation. In light of this information an attempt was made to locate the source using time-of-arrival information.

B. Correlation Analysis

Using time-of-arrival techniques to locate a source of disturbance is briefly discussed in the theory section of this report. It can be shown that if an array of three or more sensors is receiving signals from a sound source simultaneously, the essential parameter to measure is the difference between times-of-arrival of the signal at the various receiver locations (delay times). Knowing the difference between the times-of-arrival of a signal at several locations and the distance between the receivers (base line), the source of disturbance can be located from simple geometrical considerations (see Section II.B.). The most common method for determining delay times is a technique known as cross-correlation. The necessary prerequisite for this method to work is that the signal is not periodic. If the signal is periodic (see theory) the solution is not unique and the technique completely fails unless time differences less than the period of the signal are expected. This implies sensor separation less than one wavelength long. However, this restriction is operationally difficult to realize with the present IGLOO WHITE Phase III sensors. Operationally, for the present application, one works with sensor separation which is much larger than the wavelength of the

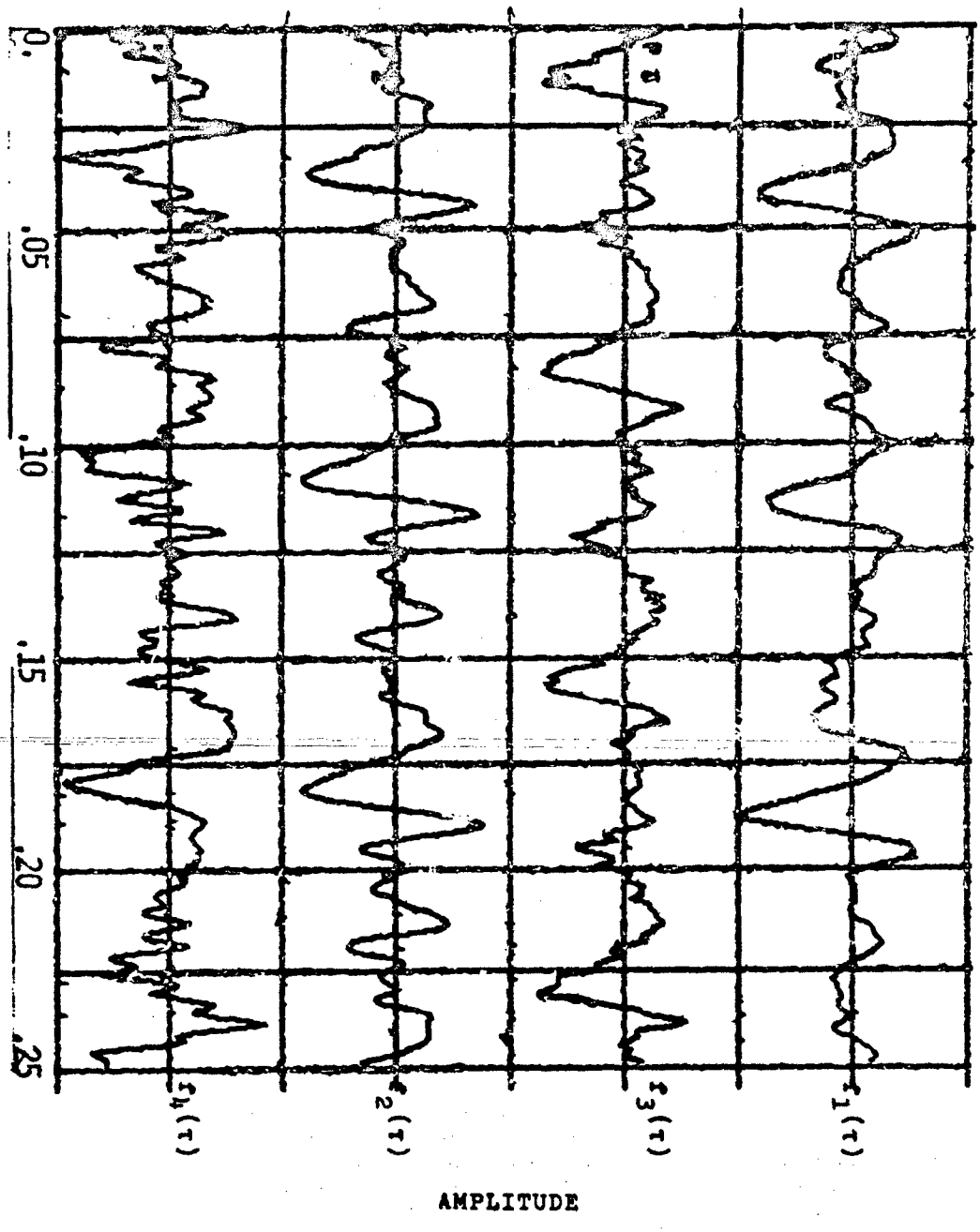

Figure 8. Time Waveform Generated by the Source as Recorded at the Four Microphones of Array Number 2

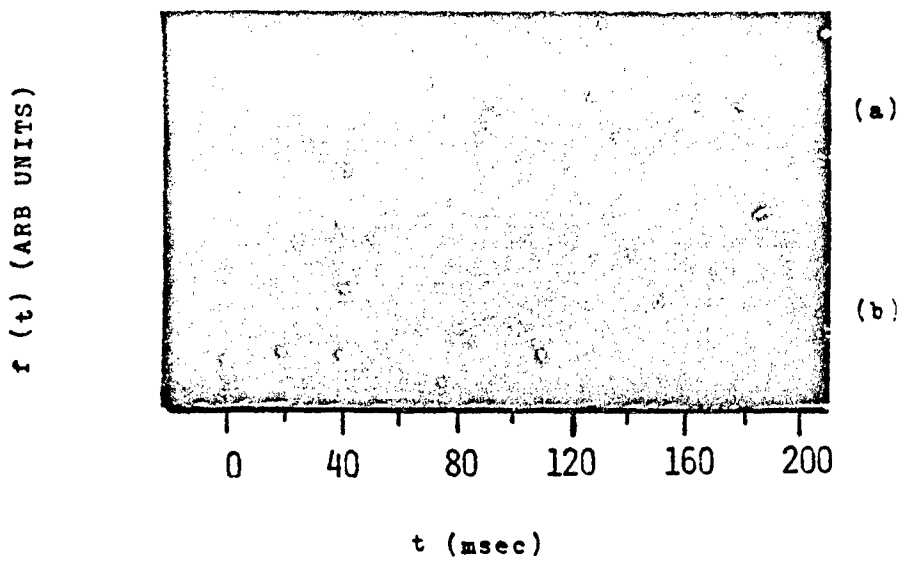

Figure 9. Time Waveform Generated by the Source: (a) exciter-on; (b) exciter-off

minimum frequency component in the "source" signal. It is therefore required that the "source" signals must contain some degree of randomness for this technique to work at all.

1. Results and Interpretation

The correlation analysis summarized here is performed using array number 4. Calculations from the other arrays are omitted since they give similar results. The different array configurations are discussed in Chapter III. Figures 11, 12, 13, 14, 15 and 16 show the correlation function that has been computed using the output from different microphones of array configuration number 4. In these figures a display of the cross-correlation function of the source (generator), the band-limited noise, and the swept tones are shown for comparison purposes.

Table I summarizes the results of this correlation analysis. The discrepancies observed between theoretical and experimental values of the delay times are believed to be due to the fact that the theoretical values were computed on the assumption that the terrain was flat. In actuality this was not the case. On the other hand, the differences observed between the calculated values of the delay times of the source and the test signals using the same microphone pair are attributed to the fact that the test signals when played back into the system were physically separated from the source by about three meters. That is, a maximum delay difference in the order of 8 milliseconds is possible. This is well within the differences observed. This point clearly shows the resolution of the technique. The good agreement between theory and experiment demonstrates that a source of disturbance can be localized with a high degree of accuracy using correlation techniques applied over long base lines.[11] The computations summarized here were performed using a Federal Scientific Correlation and Probability Analyzer.

From the above it should be noted that although in the analysis range between zero and 100 milliseconds no real difficulties existed in reducing excessive periodic components from the correlation function, in all cases it was possible to produce the true correlation maximum. The real problem for larger delays is by far more complex.

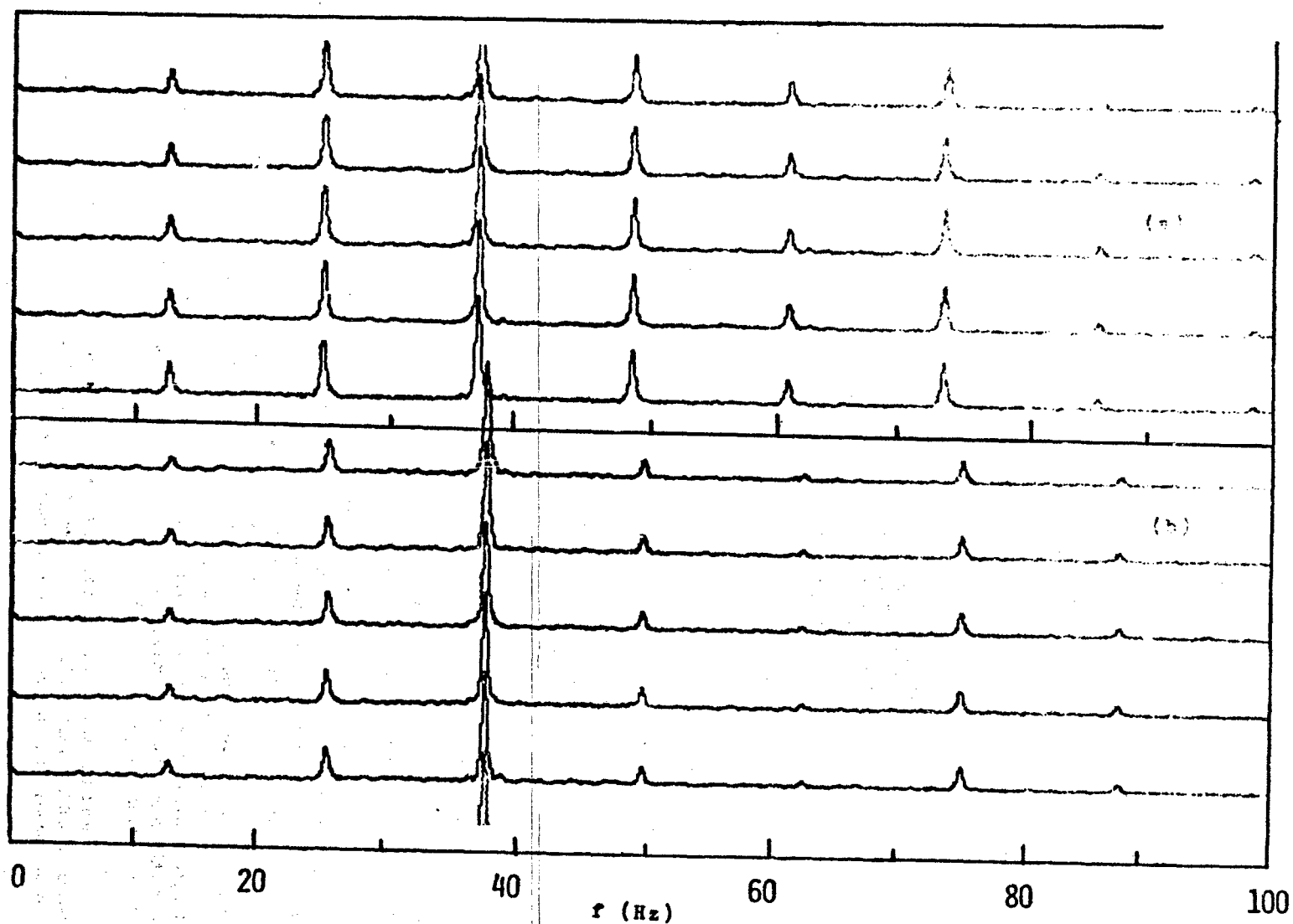

Figure 10. Time Series Spectrum of the Source Signal: (a) exciter-on; (b) exciter-off

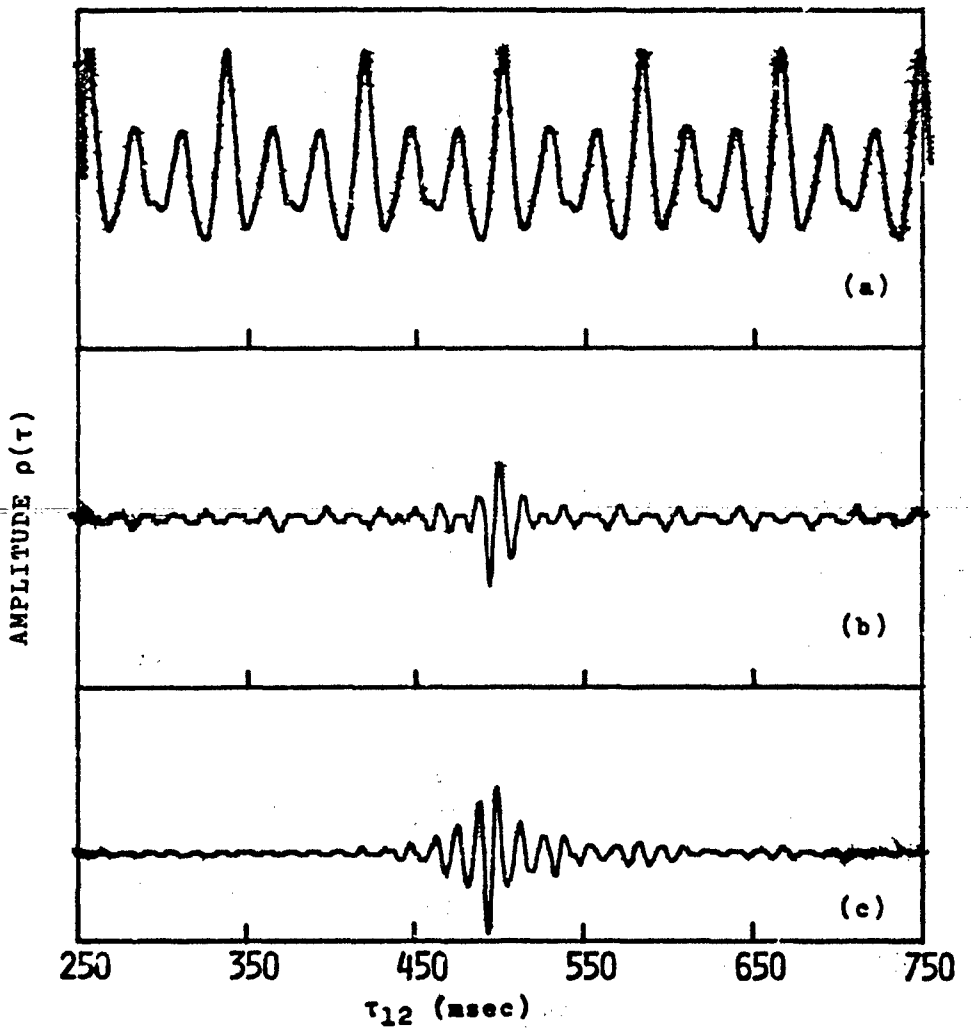

Figure 11. Cross-correlation Function of M1 vs M2: (a) source signal; (b) 40-80 Hz band-limited white noise; and (c) 40-150 Hz swept tones

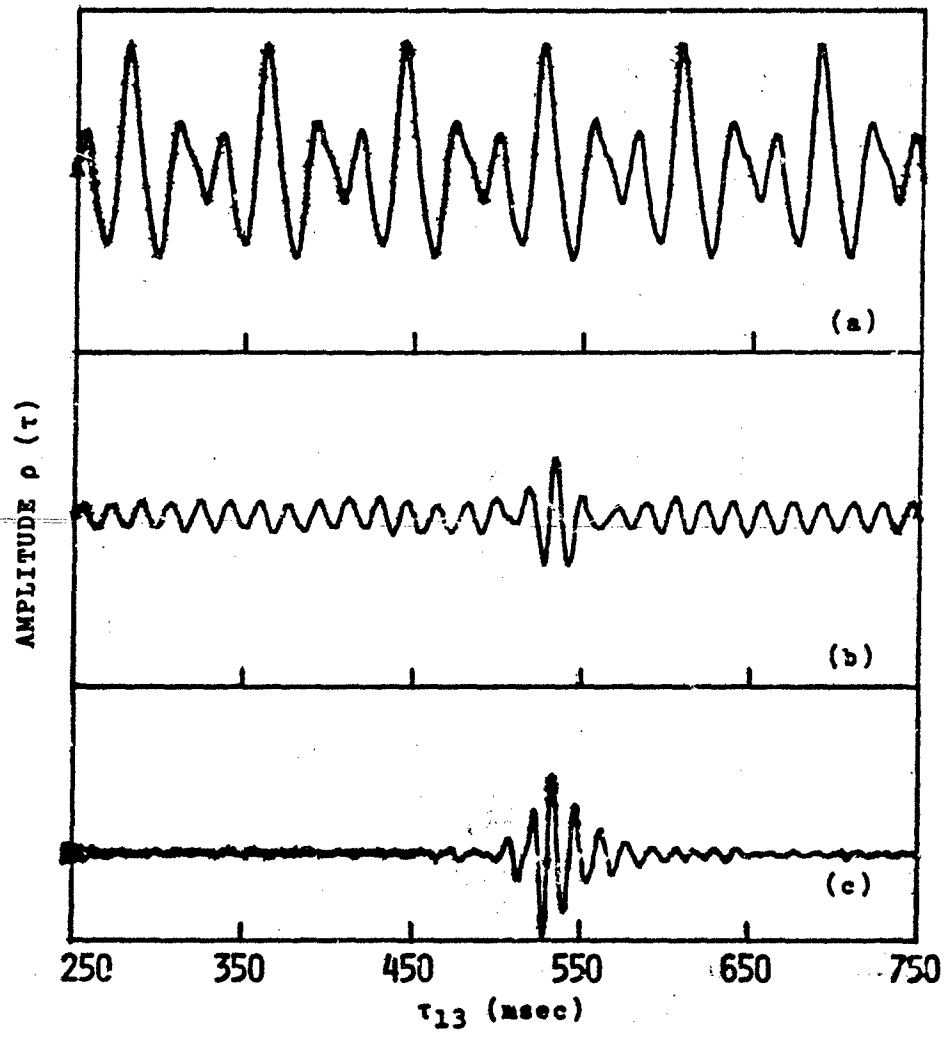

Figure 12. Cross-correlation Function of M1 vs M3: (a) source signal; (b) 40-80 Hz band-limited white noise; and (c) 40-150 Hz swept tones.

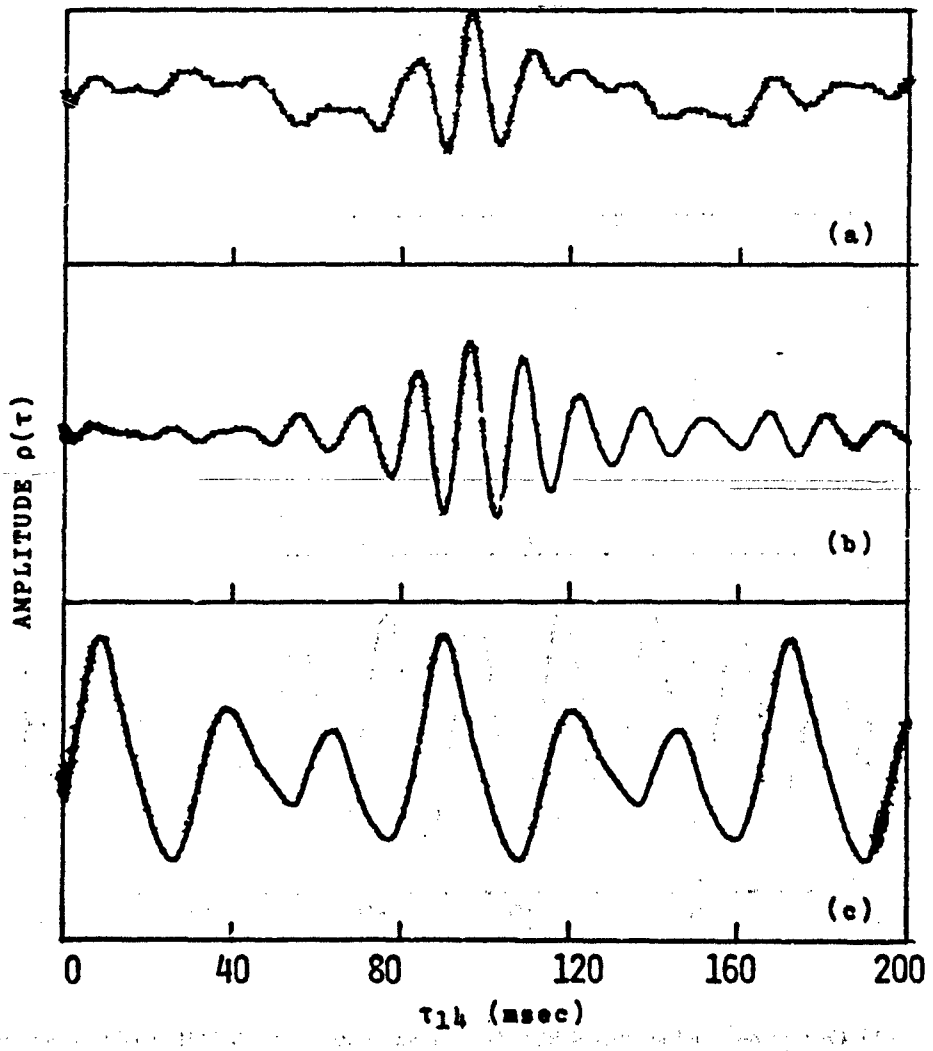

Figure 13. Cross-correlation Function of M1 vs M4: (a) 40-80 Hz band-limited white noise; (b) 40-150 Hz swept tones; and (c) source signals.

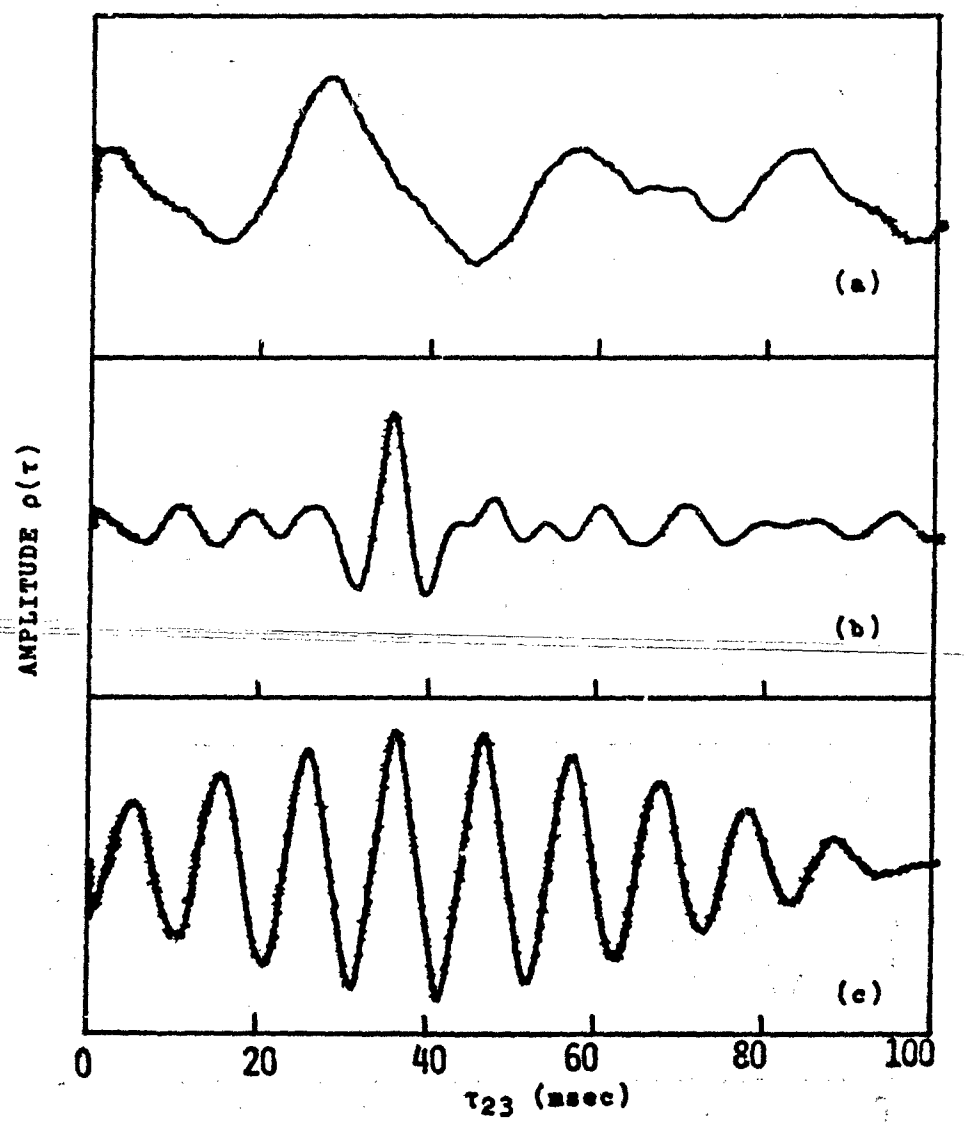

Figure 14. Cross-correlation Function of M2 vs M3: (a) source signals; (b) 40-80 Hz band-limited white noise; and (c) 40-150 Hz swept tones.

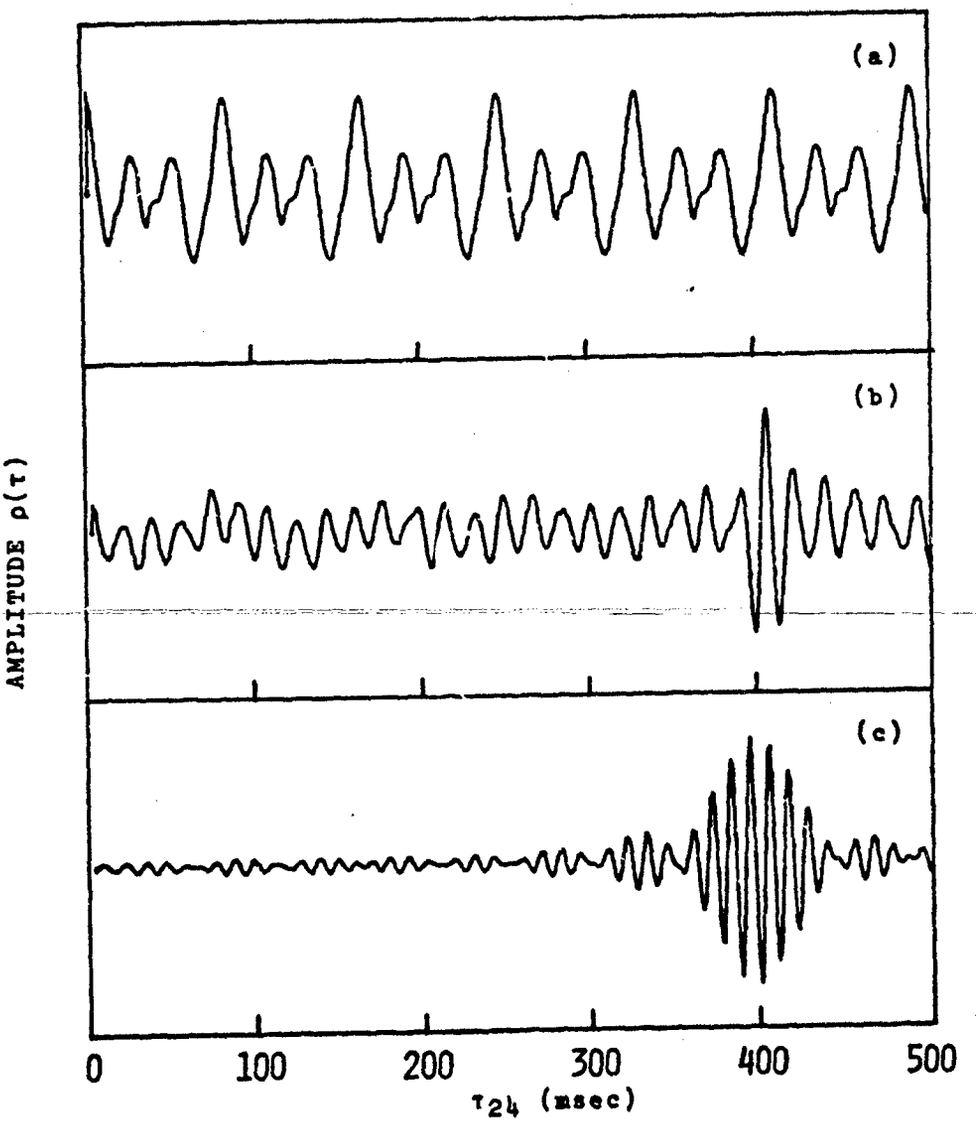

Figure 15. Cross-correlation Function of M2 vs M4: (a) source signals; (b) 40-80 Hz band-limited noise; and (c) 40-150 Hz swept tones.

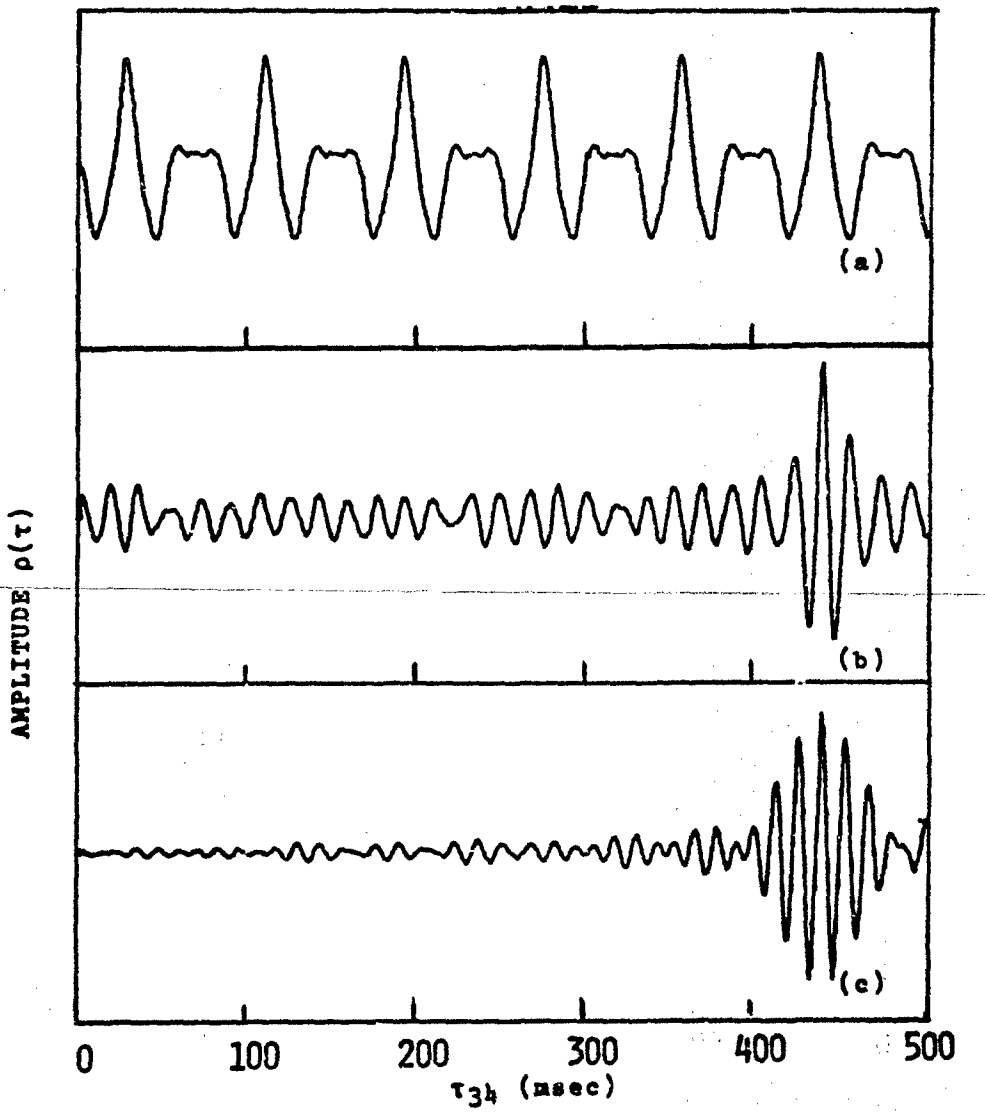

Figure 16. Cross-correlation Function of M3 vs M4: (a) source signals; (b) 40-83 Hz band-limited noise; and (c) 40-150 Kz swept tones.

TABLE I. Correlation Analysis (Array No. 4)

MICROPHONE PAIR	THEORETICAL DELAY τ (msec)	EXPERIMENTAL DELAY		
		SOURCE τ (msec)	NOISE τ (msec)	SWEPT TONES τ (msec)
M1 vs M2	510	500	500	500
M1 vs M3	536	528	535	535
M1 vs M4	78	90	96	96
M2 vs M3	26	28	36	36
M2 vs M4	432	412	408	408
M3 vs M4	458	438	442	442

When the analysis range is extended beyond the 100 milliseconds range, additional spurious peaks made it very difficult to locate the true maximum. Figures 11, 12, 13, 15, and 16 clearly demonstrate this point. In these figures the correlation functions of the source and different test signals using different microphone pairs are summarized. Notice that using the signal as it is, the additional maxima occurring every 80 milliseconds are very difficult to eliminate. These periodic maxima are due to the 12.5 Hz signal modulation whose nature is discussed in an earlier section of this report.

Faced with this dilemma two possible solutions were discussed: (a) deploy a sensor system whose base lines would be less than 30 meters; or (b) find the origin of the periodic components and determine means to reduce their effect on the correlation function. Since the first solution was very difficult to realize from the operational point of view, emphasis was placed in the area of signal processing with the possibility of extracting features (parameters) that were characteristic of the random components in the signal. This was hopefully based on the assumption that by its nature any mechanical system produces a signal which in addition to the periodic components contains also some degree of randomness. That is,

$$f(t) = ap(t) + bn(t) \tag{19}$$

where the ap(t) and bn(t) are the periodic and random parts of the emitted signal f(t). Based on this assumption the correlation function becomes,

$$R_{1,2}(\tau) = \frac{1}{2T}\int_{-T}^{T} f_1(t)\, f_2(t-\tau)\, dt = \frac{1}{2T}\int_{-T}^{T} a_1 a_2\, p_1(t).$$

$$p_2(t-\tau)dt + \frac{1}{2T}\int_{-T}^{T} b_1 b_2\, n(t)\, n(t-\tau)\, dt \tag{20}$$

The question that arises now is, what is the contribution of the second term to the correlation function? In answering this question the following analysis was performed. Over a fixed window the auto-correlation function of the source signal was computed after the signal was passed through a 100-1000 Hz high pass filter. The background signal was also auto-correlated under identical conditions. The results of this analysis are summarized in Figure 17. By comparing the two auto-correlation functions (source on/source off) it can be shown that the additional energy at τ=0 in the case of the source auto-correlation function is due to the contribution of the random components in the source signal. Notice that the 100-1000 Hz filter was used to eliminate the contribution

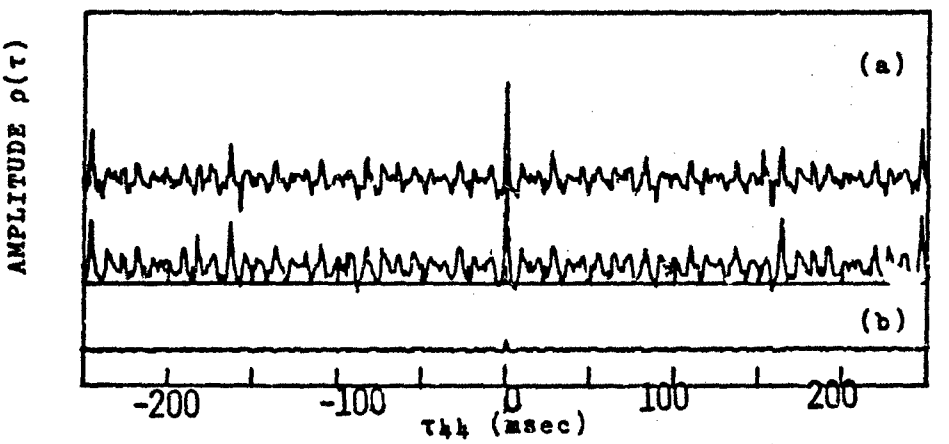

Figure 17. Auto-correlation of 100-1000 Hz band-limited: (a) source signal; (b) background noise.

of the strong periodic components of the signal that are found below 100 Hz (Figures 11 and 12). The effect of the filtering on the cross-correlation function is shown in Figure 18. For this analysis the signals of microphones M3 and M4 have been used. Notice that for the case where the 150-1000 Hz filter was used the spurious maxima have been greatly reduced and a discernible true correlation maximum is observed at τ=438 milliseconds. This figure clearly demonstrates that signal preconditioning is required before cross-correlating signals produced by generators and other generator-like targets.[10]

In addition to the above, the following analysis was performed with the help of a general purpose digital computer: (a) the computation of the normalized cross-correlation function, and (b) the computation of the cross-correlation function after prewhitening the signals. Prewhitening is used here with the intent to reduce the effect of the periodic components of the signal in the correlation function.[10] The net effect would be similar to that demonstrated in Figure 18 where special filtering techniques were applied.

Using Equation (2) and a digital computer the normalized cross-correlation function has been computed. The results of this analysis are shown in Figure 19. In the majority of the runs, although the normalized correlation function was highly periodic, the true correlation maximum was the strongest maximum in the function, as was expected. For reasons, however, that we cannot explain, in some correlation runs this was not the case. In the case of Figure 19 the signals of microphones M2 and M3 have been cross-correlated producing a maximum at τ=28 milliseconds. From array number 4 and Table I we see that this maximum corresponds to the true time difference between times-of-arrival of the source signal at microphones M2 and M3. In most of the runs, similar results were obtained between the other microphone pairs. However, since this analysis did not give reproducible results 100% of the time, it was decided to apply prewhitening techniques before the signals were cross-correlated. The theory behind the prewhitening scheme is summarized in Chapter II. The results of this analysis are shown in Figure 20.

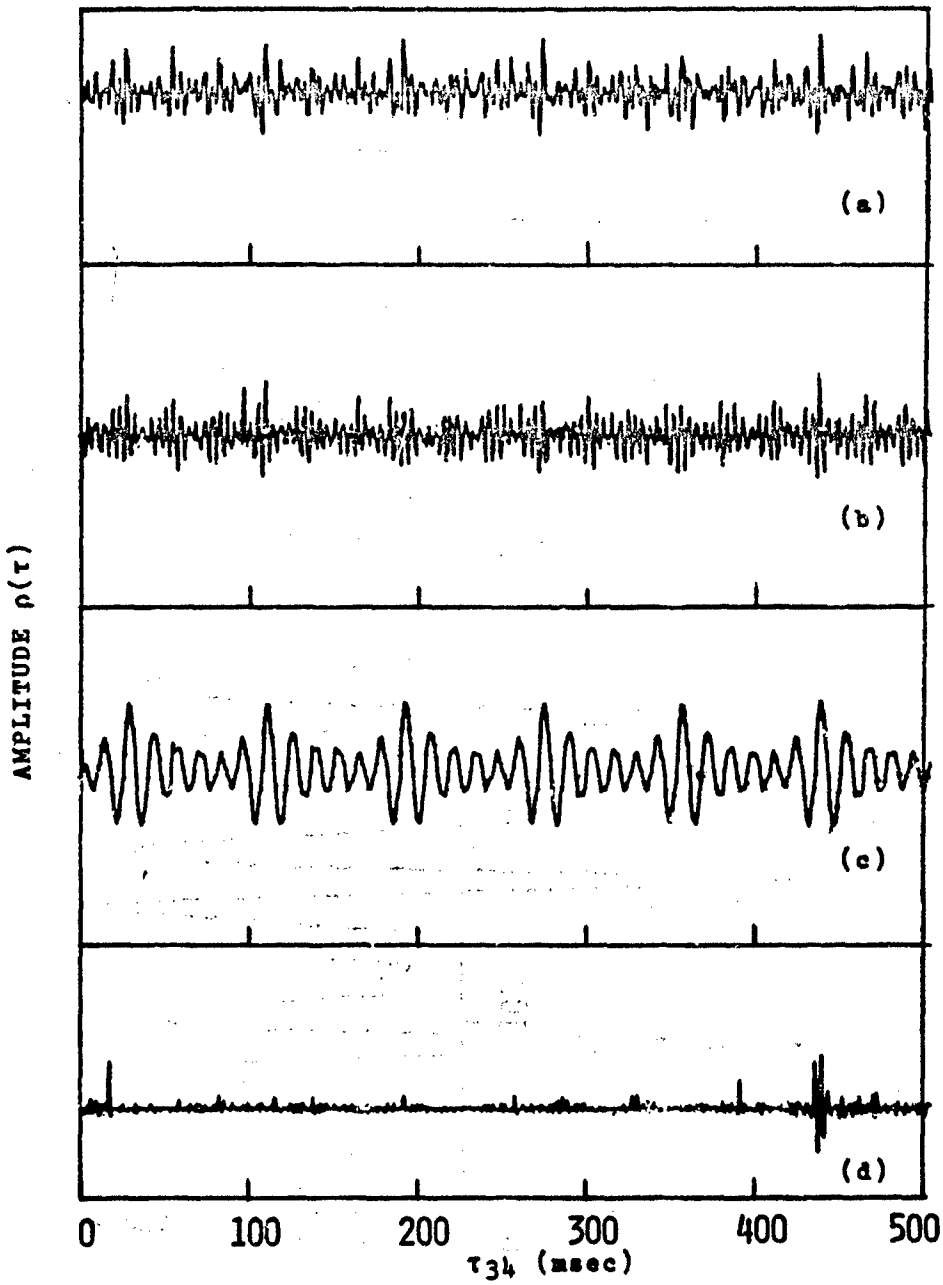

Figure 18. Cross-correlation Function of M3 vs M4 (Array No. 4) over the Analysis Range 0-500 msec. Band-Limited Source Signals: (a) 100-1000 Hz; (b) 150-1000 Hz; (c) 50-1000 Hz; and (d) band-limited white noise 160-320 Hz.

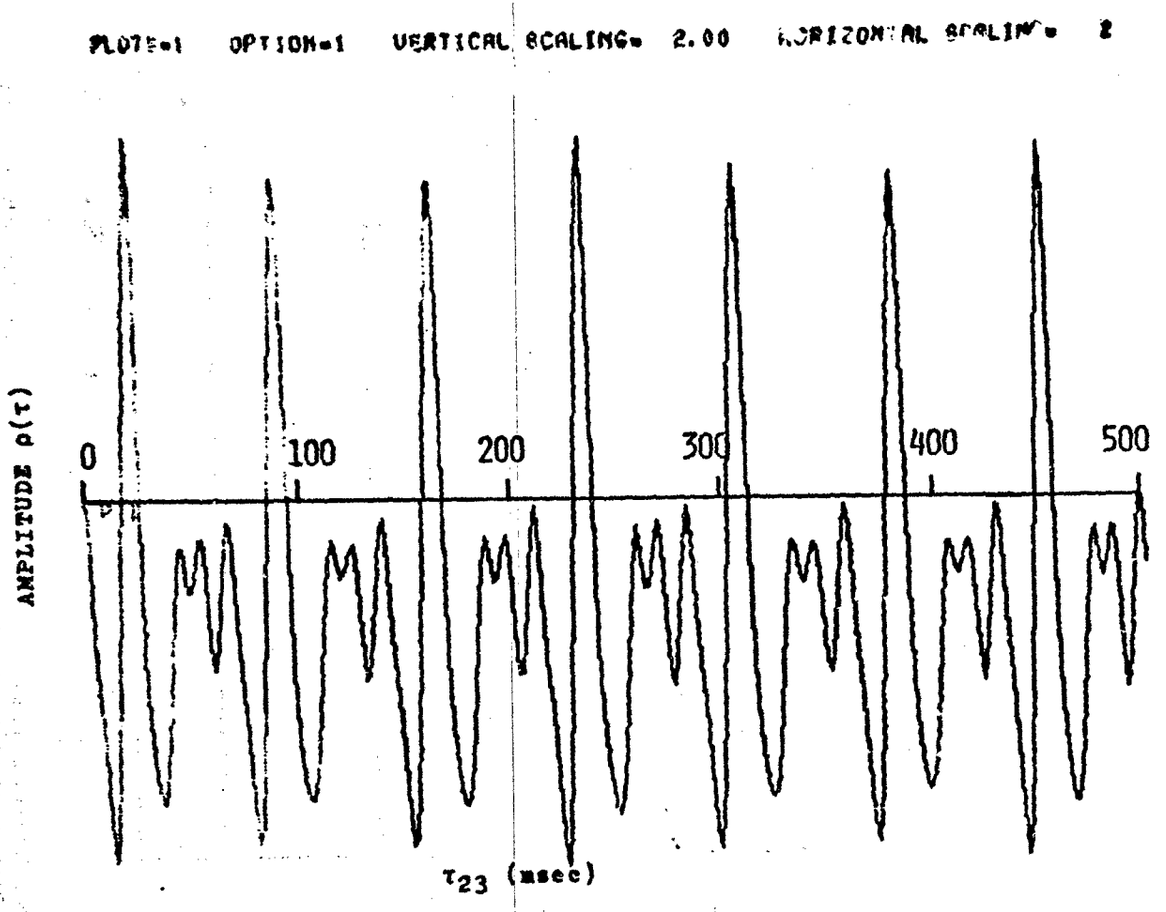

Figure 19. Normalized Cross-correlation M2 vs M3 of Unwhitened Source Signals (τ=28 msec).

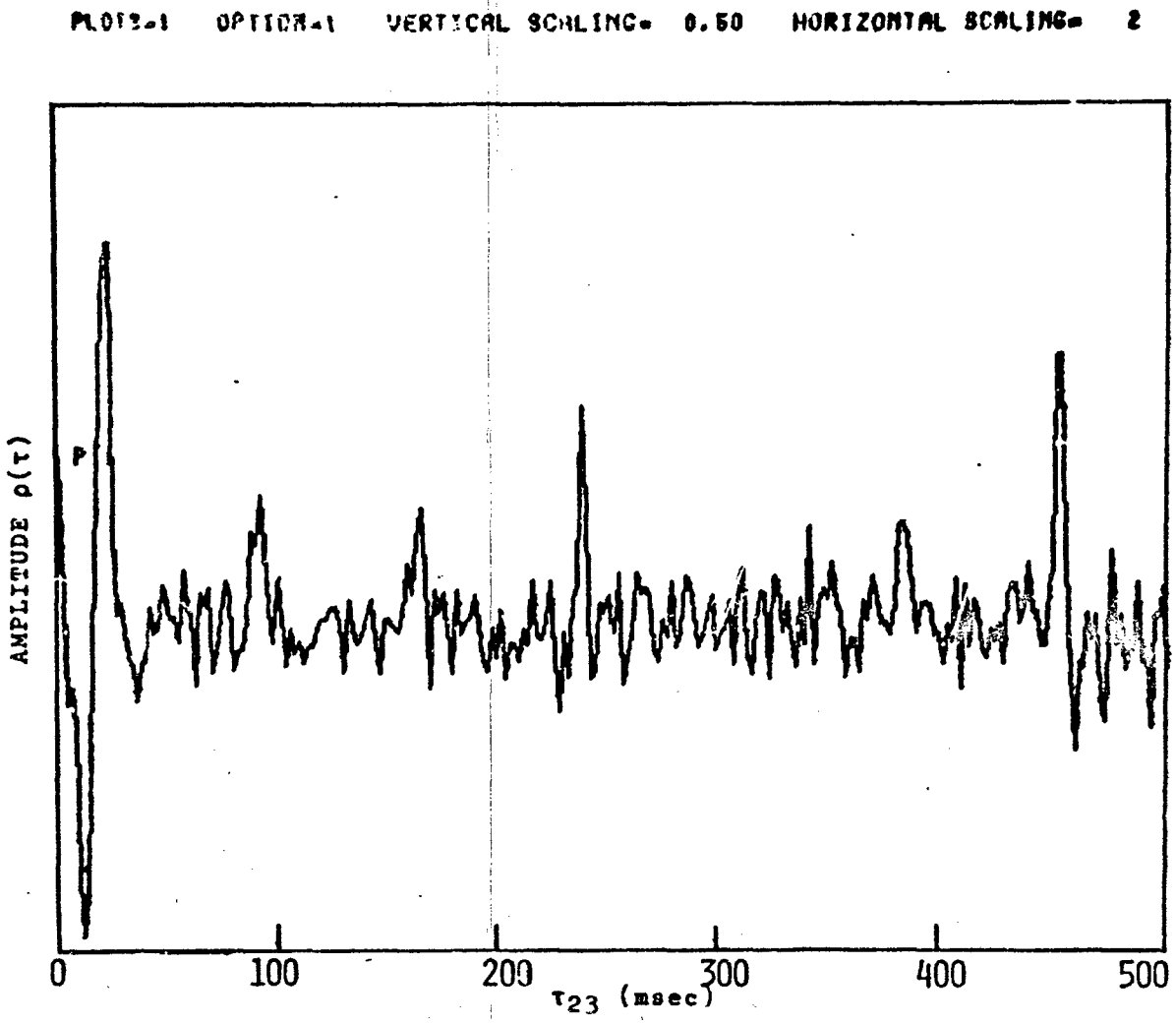

Figure 20. Normalized Cross-correlation M2 vs M3 of Log-Whitened Source Signals.

In this figure the signals of microphones M2 and M3 used to produce Figure 14 were prewhitened and then were cross-correlated. In this case, as in the one above, the maximum at τ=28 milliseconds is the true maximum and stands well above the spurious maxima. The analysis done with other pairs of microphones using prewhitening techniques as a function of integration window is shown in Figure 21. In this figure the correlation maximum is centered over the analysis window. Using this technique all computer runs produced discernible correlation maxima. On the other hand notice that the periodic component has been greatly reduced as compared to Figure 10.

Once a workable correlation technique was established an attempt was made to locate the source using data that were obtained through an operational system (see Chapter III). Although the IGLOO WHITE Phase III system filtered out most of the energy below 50 Hz because of a notch filter used at about 60 Hz (Figure 22), the correlation maximum could be found quite easily (Figure 23). Using the delay times (τ) between different microphone pairs and Equation 8 one can solve for the coordinates of the source. These results indicate that mechanical sources whose main signal is highly periodic could be located using correlation techniques.

Notice that in addition to the method described in this report for identifying the generator-type targets, a technique based strictly on looking for the engine firing rate has been successfully deployed in SEA.[19] A brief description of this type of detection is given in Chapter III of this report. For more details see reference (19).

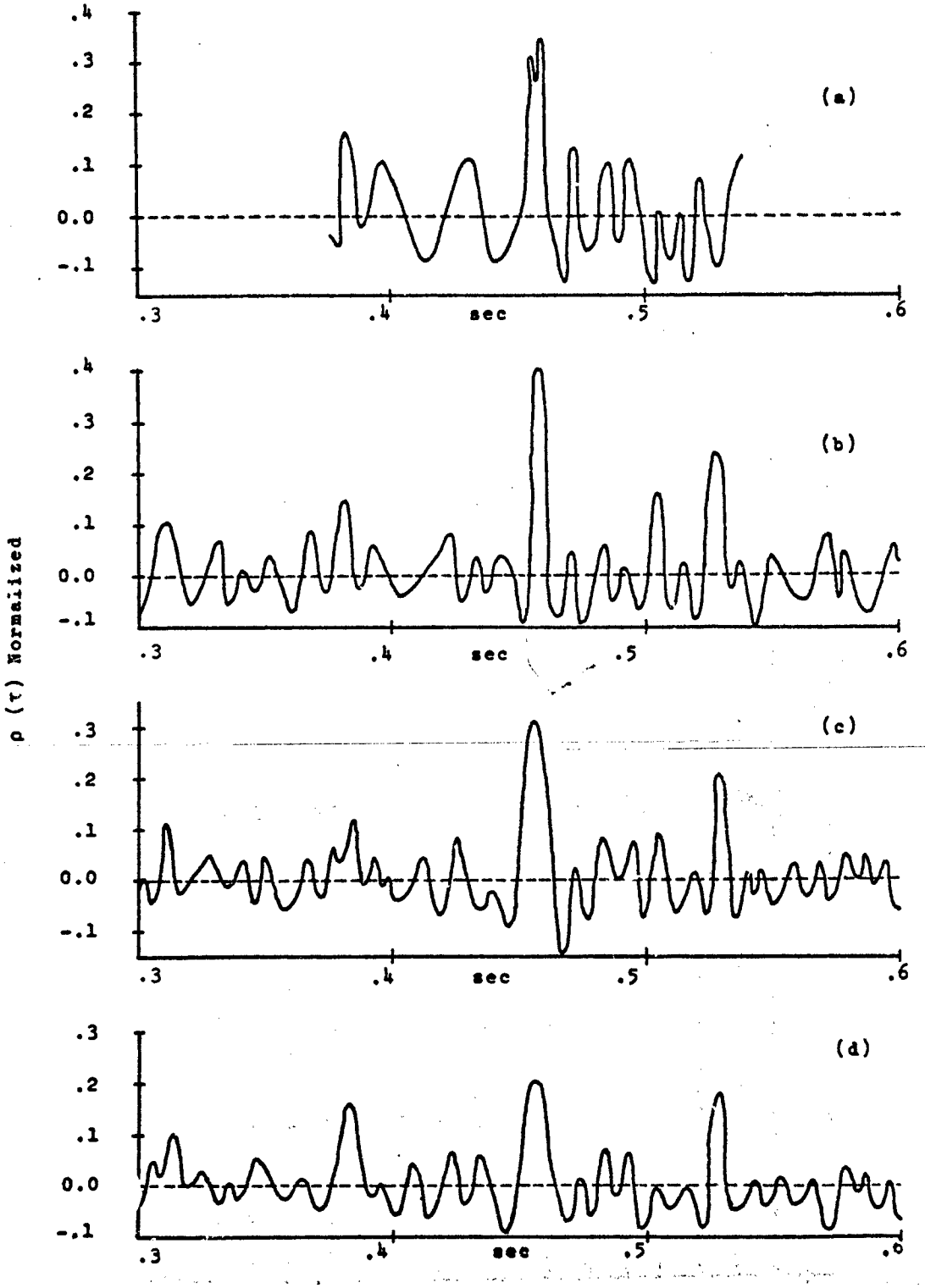

Figure 21. Cross-correlation Between M3 and M4, after Signal Prewhitening, as a Function of the Integration Windows: (a) 1/4 sec window; (b) 1/2 sec window; (c) 1 sec window; (d) 4 sec window.

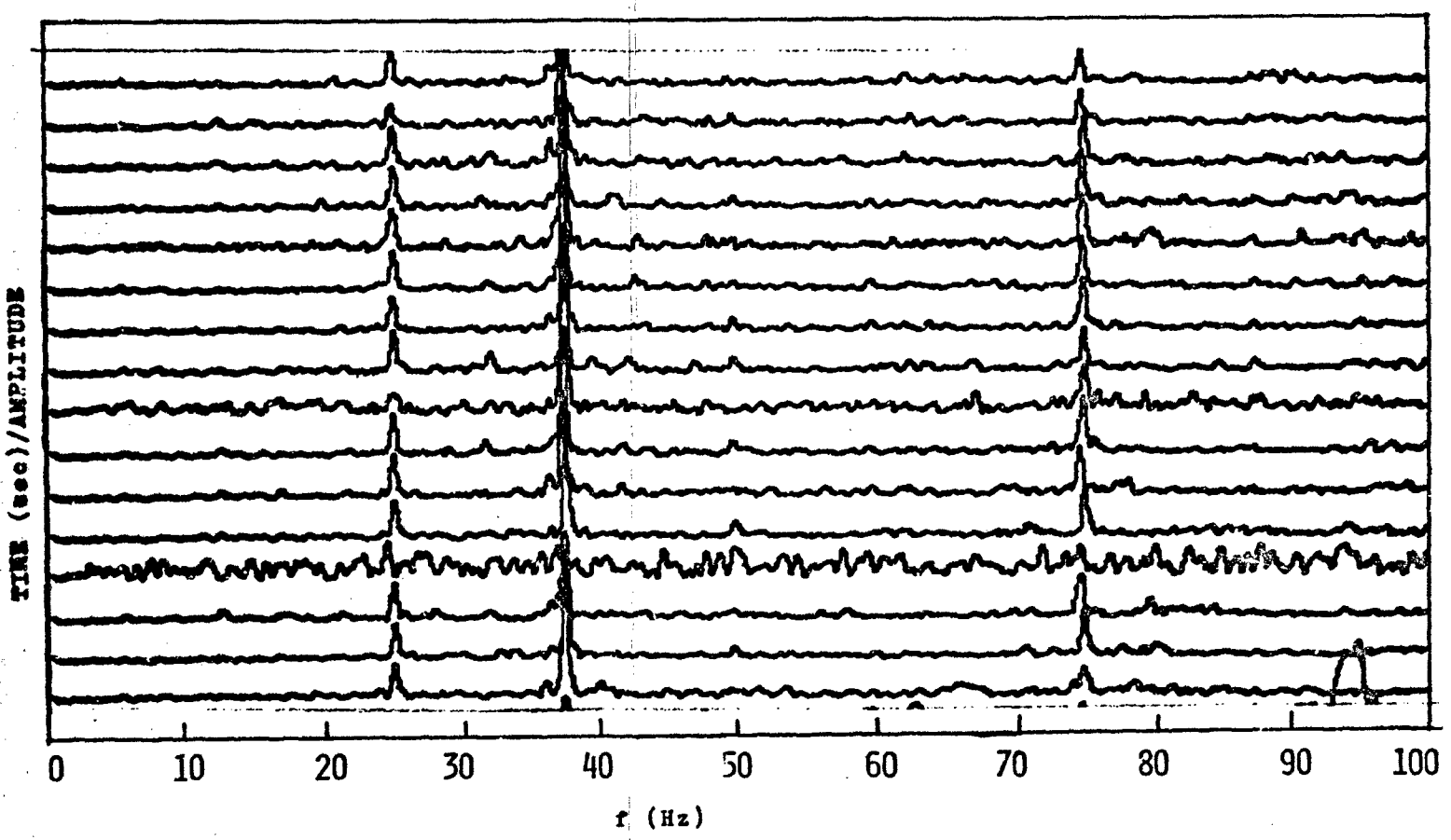

Figure 22. Time Series Spectrum of the Source Signal Using Data Obtained from an Operational System (Eglin AFB).

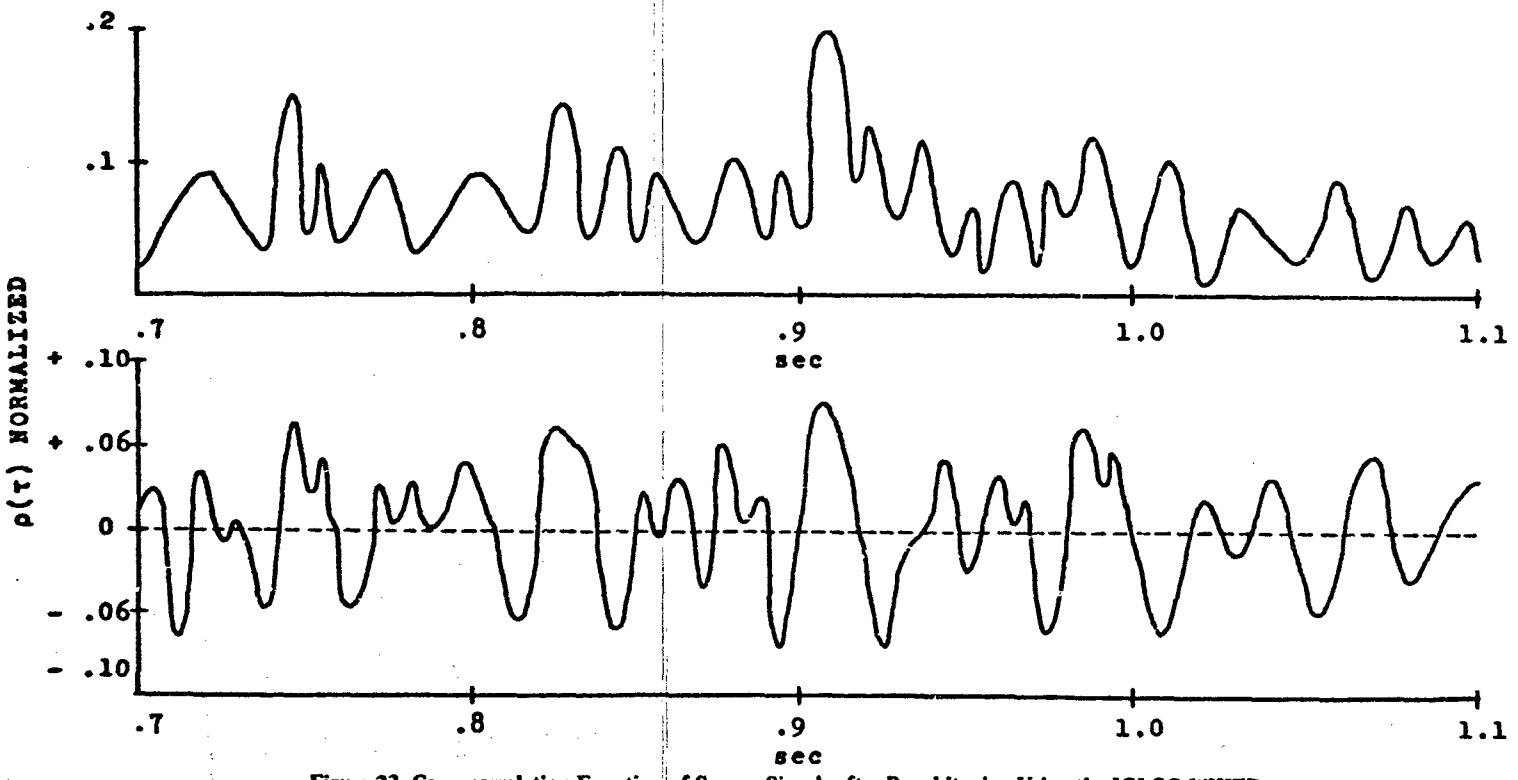

Figure 23. Cross-correlation Function of Source Signals after Prewhitening Using the IGLOO WHITE System

V. (C) Summary and Conclusions (U)

(C) This work was concerned with application of acoustic base line techniques to detection, identification, and location of enemy weapon systems powered by generators. An acoustic base line system locates by measuring time-of-arrival of acoustic signals produced by the target of interest, in this case the generator, at three or more acoustic sensors distributed in a relatively broad array. Such time-of-arrival (TOA) techniques have been used successfully in other applications. In this case, however, the long base line (acoustic sensor separation) and the highly periodic nature of acoustic signals generated by the source lead to severe ambiguity in source location. The technical challenge in this work involved separation of the periodic components of the source signals and preservation of the more random components for use in arrival time measurement and subsequent target location.

(C) Experimental work was performed at Eglin AFB, Florida and was designed to provide information on all variables of interest including weather and interference. The sources used were:

1. Foreign generators
2. Pure and swept tones
3. Band-limited white noise
4. Explosions
5. Aircraft interference
6. Vehicles singly and in groups.

(C) Detection was performed using the following:

1. Hard-wired microphones wired into an RADC recording facility.

2. Existing IGLOO WHITE system with Phase III modified commike collocated with RADC microphones.

All aspects of the experiment including design, installation, and operation of the instrumentation system were performed by RADC personnel with support from 3246TW, Eglin AFB, Florida.

(C) Subsequent to the field phase of the program, the data were analyzed at RADC using correlators, spectrum analyzers, and digital data processing equipment. The results of the analysis successfully demonstrated the following:

1. Detection and location of the source was possible over base lines of 600 meters by applying:
   a. Signal prewhitening techniques; and/or
   b. Stochastic correlation techniques.
2. Accuracies within a few meters were achieved under calm weather conditions.
3. Identification of the target was performed based on the modulation of the acoustic signal by the fundamental frequency of the source.

(C) The technique described above provides an approach to remote monitoring of enemy lines of communications and fixed installations for tactical target interdiction and strategic purposes. The most important current example is location of SAM generators in a jungle environment. Presently this type of source is very difficult to locate using other detection techniques. This work not only provides a tool for accurately locating SAM generators with available hardware, it also provides the means for properly classifying the target.

REFERENCES

1. Faron, Jr., J.J. and Hills, Jr., R., "The Application of Correlation Techniques to Acoustic Receiving Systems," Technical Memo No. 27 and 28, Acoustic Research Laboratory, Harvard University, Cambridge, Mass., 1952.

2. Goff, K.W., "The Application of Correlation Techniques to Some Acoustic Measurements," *J. Acoustical Soc AM* 27, 236, 1955.

3. Lange, F.H., *Correlation Techniques*, Iliffe Books Ltd., 1967.

4. Gilbrech, D.A., and Binder, R.C., "Portable Instrument for Locating Noise Sources in Mechanical Equipment," *J. Acoustical Soc Am* 30, 842, 1958.

5. Jacobson, M.D., and Talham, R.J., "Use of Pressure Gradient Receivers in a Correlator Receiving System," *J. Acoustical Soc Am* 31, 1352, 1959.

6. Jacobson, M.J., "Correlation of a Finite Distance Point Source," *J. Acoustical Soc Am* 31, 448, 1959.

7. Jacobson, M.J., "Space-Time Correlation in Spherical and Circular Noise Fields," *J. Acoustical Soc Am* 34, 971, 1962.

8. Bolt, Beranek and Newman, Inc., "Signal Processing Techniques for Sound Ranging," Technical Reports ECOM-0378-1, 1967; ECOM-0378-3, 1968; ECOM-0378-4, 1969.

9. Harris, J.R., "Study of Sound Location by Hyperbolic Fixing," NADC-SD-6814, 1968.

10. Maloney, J.E., Sebastian, R.L., and Mathieu, K.F., "Evaluation of Atmospheric Correlation Techniques," RADC-TR-72-179, 1972, AD 903 724.

11. Constantine, J.G. and Dickinson, M., "Long Base Line Acoustic Correlation Techniques," RADC-TR-72-265, 1972, AD 906 705.

12. Willow Run Laboratories, "An Investigation of Factors Affecting Sound Ranging; Literature Research and Analysis," The Institute of Science and Technology, University of Michigan, AD 698 565, 1969; AD 711 574, 1970; AD 711 575, 1970; and ECOM-00013-209, 1971.

13. Papoulis, A., *Probability, Random Variables and Stochastic Processes*, McGraw-Hill Book Company, 1965.

*14. Defense Special Projects Group, "DSPG Systems Design Description," 20 August 1971, Secret, Group 3.

15. Fountain, L.S., "The Influence of Meteorological Conditions on the Propagation of Ultrasonic Energy in Air Near the Earth's Surface," Special Research Report, Southwest Research Institute, May 1962.

16. Fountain, L.S., Owen, E.T., and Vest, Wid, "Development and Evaluation of the Sonic Intrusion Detector," Final Report, February 1969, AD 500 196.

17. Eyring, C.F., "Jungle Acoustics," *J. Acoustical Soc Am* 18, 257, 1946.

18. Torok, S.F., "Vehicle, Aircraft Classification Manual," Naval Air Development Center, NADC-72058-SD, 21 April 72.

*19. AFSC, Eglin AFB, FA, "Evaluation of Modified COMMIKE," Project Directive No. 0125A001, Headquarters, 3246th Test Wing, 12 Mar. 72, Secret, Group 3.

APPENDIX

The time domain correlation program was written in FORTRAN IV for use on a PDP-9 general purpose digital computer by RADC/DCTI. The correlation function is normalized (Eq 2) and printed out in integer format. A plot of the normalized correlation function can be obtained by a software plotting program.

The correlation program has the capability of handling 835 points per correlation. The resolution depends on the digitizing rate of the data in conjunction with the 835 point per correlation.

The three-sensor target location program was also written in FORTRAN IV by RADC/DCTI. The array geometry and the time delays of the acoustic signatures of interest between the three sensors are needed for a location.

The general equations used in the digital program for the three-sensor target location using TOA are:

$$V_0 \tau_{12} = (X_0^2 + Y_0^2)^{1/2} - [(X_0 - X_2)^2 + (Y_0 - Y_2)^2]^{1/2} \tag{21}$$

$$V_0 \tau_{13} = (X_0^2 + Y_0^2)^{1/2} - [(X_0 - X_3)^2 + (Y_0 - Y_3)^2]^{1/2} \tag{22}$$

where

V_0 - speed of sound.

τ_{12} - Delay time for the acoustic signature of interest between sensor 1 and sensor 2.

τ_{13} - Delay time for the acoustic signature of interest between sensor 1 and sensor 3.

X_0, Y_0 - Cartesian coordinates of the target location.

X_2, Y_2 - Cartesian coordinates for sensor 2.

X_3, Y_3 - Cartesian coordinates for sensor 3.

The location of sensor 1 is at the origin of the Cartesian coordinate system, therefore $X_1 = 0$ and $Y_1 = 0$.

Solving for the target location, the following equations are obtained:

$$X_0 = A + BR_0 \tag{23}$$

$$Y_0 = A_1 + B_1 R_0 \tag{24}$$

where

$$R_0 = (X_0^2 + Y_0^2)^{1/2} \tag{25}$$

$$A = \frac{Y_3 (X_2^2 + Y_2^2) - Y_2 (X_3^2 + Y_3^2) - Y_3 (V_0 \tau_{12})^2 + Y_2 (V_0 \tau_{13})^2}{2 (X_2 Y_3 - X_3 Y_2)} \tag{26}$$

$$B = \frac{Y_3 (V_0 \tau_{12}) - Y_2 (V_0 \tau_{13})}{X_2 Y_3 - X_3 Y_2} \tag{27}$$

$$A_1 = \frac{X_2 (X_3^2 + Y_3^2) - X_3 (X_2^2 + Y_2^2) + X_3 (V_0 \tau_{12})^2 - X_2 (V_0 \tau_{13})^2}{2 (X_2 Y_3 - X_3 Y_2)} \tag{28}$$

$$B_1 = \frac{X_2 (V_0 \tau_{13}) - X_3 (V_0 \tau_{12})}{X_2 Y_3 - X_3 Y_2} \tag{29}$$

Squaring equations (23) and (24), then adding the two equations together, the following quadratic solution for R_0 is formed:

$$R_0 = \frac{-J \pm \sqrt{J^2 - 4NK}}{2N} \tag{30}$$

where

$$J = 2 (AB + A_1 B_1) \tag{31}$$

$$N = B^2 + B_1^2 - 1 \tag{32}$$

$$K = A^2 + A_1^2 \tag{33}$$

As long as the target is within the triangle formed by the three sensors, a unique solution is obtained from equation (30). R_0 is then substituted into equations (23) and (24) for the Cartesian coordinate of the target location relative to sensor 1.

The block diagram of Figure 24 depicts the steps involved when signal prewhitening is used to reduce the periodic structure of the correlation function. The theory and equations used to develop the digital computer programs for signal prewhitening are described and presented in Section II.C. Below is a description of the symbols in the block diagram of Figure 24.

$X_1 (t)$, $X_2 (t)$ – Time varying functions

$F_1 (\omega)$, $F_2 (\omega)$ – Discrete Fourier transform of $X_1 (t)$ and $X_2 (t)$ respectively.

$F_2^* (\omega)$ – Complex conjugate of $F_2 (\omega)$.

$K^2 (\omega)$ – Prewhitening functions

FFT – Fast Fourier Transform

$\rho_{1,2} (\tau)$ – Cross-correlation function

WSF – Window Shaping Function (i.e. Hanning, Hamming etc.).

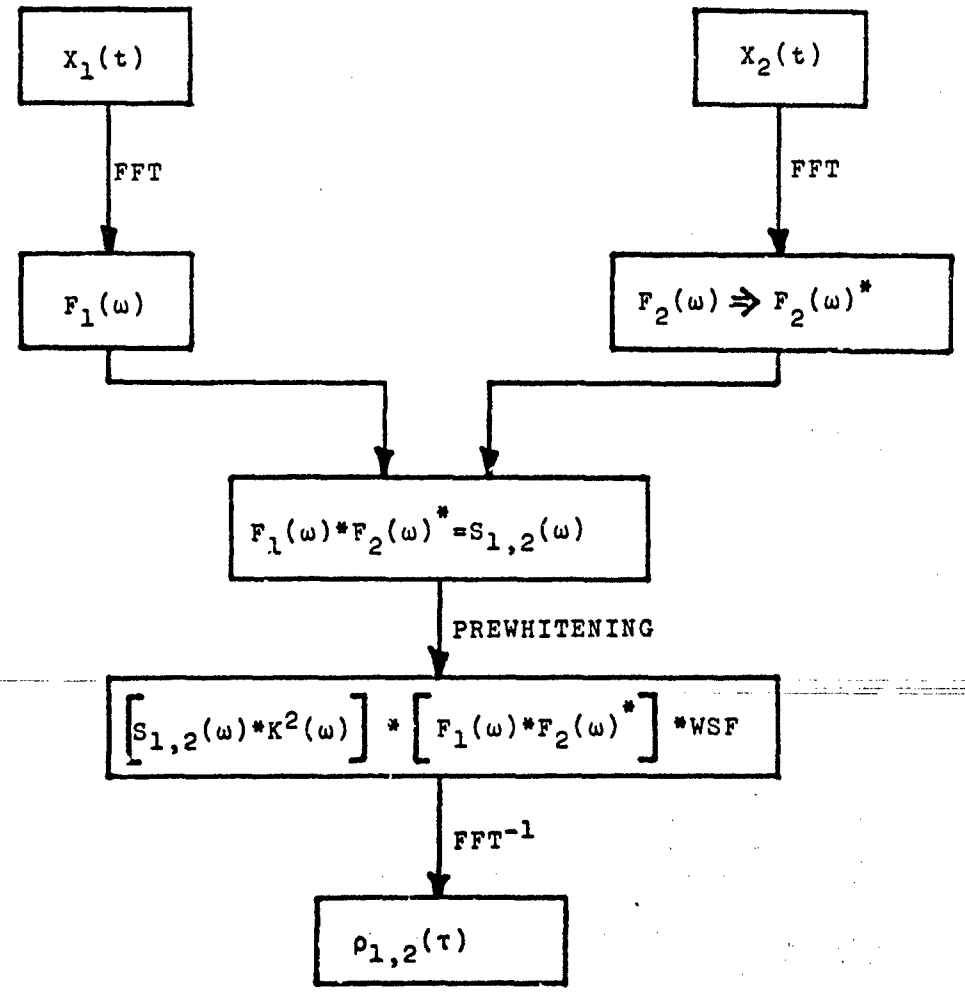

Figure 24. Block Diagram of Digital Prewhitening Technique as Applied to the Cross-Spectral Power Density

```
C     THREE SENSOR TARGET LOCATION PROGRAM.
C     ROME AIR DEVELOPMENT CENTER.
C     LT MARK D. DICKINSON (DCTI).
C
C
C     CALL INIT INITIALIZES THE TEKTRONIX 611 DISPLAY.
      CALL INIT
C     READ IN ARRAY DIMENSIONS AND TIME DELAYS FOR THREE SENSORS.
101   FORMAT (F8.3)
200   WRITE (4,100)
100   FORMAT (38H DISTANCE BETWEEN M1 AND M2 IN METERS:)
      READ (4,101) R12
      WRITE (4,102)
102   FORMAT (38H DISTANCE BETWEEN M1 AND M3 IN METERS:)
      READ (4,101) R13
      WRITE (4,104)
104   FORMAT (34H ANGLE FROM R12 TO R13 IN DEGREES:)
      READ (4,101) TH13
      WRITE (4,106)
106   FORMAT (35H ENTER D12, D13 AND D23 IN SECONDS:)
      READ (4,300) D12, D13, D23
300   FORMAT (3F8.3)
107   FORMAT (F8.5)
C     CONVERT TH13 FROM DEGREES TO RADIANS.
      TH13=TH13*.01745
C     CONVERT TIME DELAYS FROM TIME TO DISTANCE BY
C     MULTIPLYING BY THE SPEED OF SOUND.
      D12=D12*344.
      D13=D13*344.
      D23=D23*344.
      X13=R13*COS(TH13)
      Y13=R13*SIN(TH13)
C     THREE SENSOR TARGET LOCATION COMPUTATION STARTS HERE USING
C     TIME DELAYS D12 AND D13.
      A=((R12**2)-(D12**2))/(2.*R12)
      B=D12/R12
      A1=(X13*((D12**2)-(R12**2))-R12*((D13**2)-(R13**2
      1)))/(2.*R12*Y13)
      B1=(D13*R12-D12*X13)/(R12*Y13)
      ZAP=SQRT(((2.*(A*B+A1*B1))**2)-(4.*(B**2+B1**2-1.
      1)*(A**2+A1**2)))
      RS1=(-2.*(A*B+A1*B1)+ZAP)/(2.*(B**2+B1**2-1.))
      RS2=(-2.*(A*B+A1*B1)-ZAP)/(2.*(B**2+B1**2-1.))
      IF(RS1.LE.0.) GO TO 103
      X1=A1+B1*RS1
      Y1=A+B*RS1
      THS1=(ATAN2(X1,Y1))*57.29
```

```
C     WRITE OUT DISTANCE FROM SENSOR ONE (M1) TO THE
C     TARGET LOCATION IN METERS.
      WRITE (8,105) RS1
105   FORMAT (21H+DISTANCE TO TARGET =, E14.5)
C     WRITE OUT ANGLE THS1 IN DEGREES FROM R12 TO RS1.
      WRITE (8,109) THS1
109   FORMAT (23H+ANGLE FROM R12 TO RS=,E14.5)
103   IF(RS2.LE.0.) GO TO 108
      X2=A1+B1*RS2
      Y2=A+B*RS2
      THS2=(ATAN2(X2,Y2))*57.29
      WRITE (8,105) RS2
      WRITE (8,109) THS2
C     THREE SENSOR TARGET LOCATION COMPUTATION STARTS
C     HERE USING TIME DELAYS D21 AND D23.
108   IF(RS1.LE.0.AND.RS2.LE.0.) GO TO 113
      D21=D12
      R23=SQRT((R13**2)+(R12**2)-(2.*R13*R12*COS(TH13)))
      TH21=ATAN2(Y13,(R12-X13))
      X21=R12*COS(TH21)
      Y21=R12*SIN(TH21)
      AP=(R23**2-D23**2)/(2.*R23)
      BP=D23/R23
      A1P=(X21*((D23**2)-(R23**2))-R23*((D21**2)-(R21**2)
      1))/(2.*R23*Y21)
      B1P=(D21*R23-D23*X21)/(R23*Y21)
      ZAP=SQRT(((2.*(AP*BP+A1P*B1P)**2)-(4.*(B**2+
      1B1P**2-1.)*(AP**2+A1P**2)))
      RS1P=(-2.*(AP*BP+A1P*B1P)+ZAP)/(2.*(BP**2+B1P**2-1.))
      RS2P=(-2.*(AP*BP+A1P*B1P)-ZAP)/(2.*(BP**2+B1P**2-1.))
      IF(RS1P.LE.0.) GO TO 110
      THS1P=(ATAN2((A1P+B1P*RS1P), (AP+BP*RS1P)))*57.29
      WRITE (8,105) RS1P
      WRITE (8,201) THS1P
201   FORMAT (23H+ANGLE FROM R23 TO RS=,E14.5)
110   IF(RS2P.LE.0) GO TO 112
      THS2P=(ATAN((A1P+B1P*RS2P),(AP+BP*RS2P)))*57.29
      WRITE (8,105) RS2P
      WRITE (8,201) THS2P
102   IF(RS2P.LE.0.. AND.RS1P.LE.0.) GO TO 113
      GO TO 114
113   WRITE (8,202)
202   FORMAT (26H+NO SOLUTION WAS OBTAINED.)
114   PAUSE 10
      IF(ISENSW(17).EQ.-1) GO TO 200
      STOP
      END
```

```
C     TIME DOMAIN CORRELATION PROGRAM.
C     ROME AIR DEVELOPMENT CENTER.
C     CAPT MIKE CRONE (DCTI)
C
C     SUBROUTINE CORAL
      COMMON IN(4,1670),NREC,NP
C     IN(4,1670-WORKING ARRAY WHERE ROW 1 IS THE
C               FIRST CHANNEL OF DATA, ROW 2 IS THE
C               SECOND CHANNEL OF DATA AND ROW
C               3 IS WHERE THE NORMALIZED CROSS-
C               CORRELATION IS STORED.  THE ARRAY WILL
C               HANDLE 1670 POINTS PER ROW.
C     NREC-NUMBER OF RECORDS.
C     NP=NUMBER OF  POINTS.
      B=0
      NP=NP/2
      DO 100 I=1,NP
      C=IN(1,I)
100   B=B+C**2
      DO 200 J=1,NP
      A1=0
      D=0
      DO 10 K=1,NP
      R1=In(1,N)
      L1=K+J
      R2=IN(2,L1-1)
      A1=R1*R2+A1
10    D=R2**2+D
200   IN(3,J)=A1/SQRT(B*D)*2047.
      CALL INIT
C     CALL INIT INITIALIZERS THE CRT DISPLAY.
      WRITE (8,150)
150   FORMAT (30H NORMALIZED CROSS-CORRELATION=)
      WRITE (8,175) (IN(3,J),J=1,NP)
175   FORMAT (1H,10I6)
      PAUSE 1
      RETURN
      END
```